DEPARTMENT OF THE NAVY

DAVID TAYLOR MODEL BASIN
WASHINGTON, D.C.

HYDROMECHANICS

AERODYNAMICS

STRUCTURAL MECHANICS

APPLIED MATHEMATICS

ACOUSTICS AND VIBRATION

A COMPARISON OF THE LIFTING-SURFACE CORRECTIONS CALCULATED BY DIFFERENT METHODS FOR THREE PROPELLER DESIGNS

by

Ernest E. Harley

HYDROMECHANICS LABORATORY

RESEARCH AND DEVELOPMENT REPORT

September 1965 Report 2049

A COMPARISON OF THE LIFTING-SURFACE CORRECTIONS CALCULATED BY DIFFERENT METHODS FOR THREE PROPELLER DESIGNS

by

Ernest E. Harley

September 1965

Report 2049
S-R009-01-01

TABLE OF CONTENTS

LIST OF FIGURES

LIST OF TABLES

NOTATION

A	Area of blade section
D	Diameter of propeller
EAR	Expanded area ratio
G	Nondimensional circulation per blade, $= \Gamma / 2\pi r V_a$
ℓ	Blade section length
M	Ordinate of the mean line
$\frac{M}{m_x}$	Nondimensional section mean line ordinate
M_x	Maximum camber of mean line
$\frac{M_{x3}}{\ell}$	Section camber ratio
$\frac{M_{x3}}{M_{x2}}$	Camber correction coefficient
P/D	Pitch ratio
R	Propeller radius
r	Propeller blade section radius
V_a	Speed of advance
$\frac{x}{\ell}$	Nondimensional chord position
z	Number of blades
$\alpha_i(1)$	Angle of attack due to lifting-surface effects, Kerwin's vortex lattice method, $\alpha_i^{(1)} = (P.F.)\ (C_L)\ 57.3$
$\alpha_i^{(2)}$	Angle of attack due to lifting-surface effects, Pien's continuous design method, $\alpha_i^{(2)} = \tan^{-1} \frac{M_{1.0}}{\ell}$
α_t	Angle of attack due to thickness effects, Kerwin's vortex-lattice method
$\alpha_{i_{2D}}$	$1.54\ C_L$

ABSTRACT

This report presents the results of a comparison of lifting-surface corrections calculated by several numerical methods for three propellers. Specifically, the camber corrections, radial and chordwise distribution of camber, and the propeller pitch ratios are compared. The results of the comparison, presented in nondimensional form, are shown graphically and through tables.

ADMINISTRATIVE INFORMATION

This work was done under BuShips Sub-Project S-R009-01-01, Task 0101, General Hydromechanics Research Program.

INTRODUCTION

For the past twenty years theoretical propeller design methods have had as their basis the lifting-line theory with more or less approximate corrections to account for lifting-surface effects. Investigations have shown that these corrections are not completely reliable and have pointed out a need for a more sophisticated lifting-surface correction. Before the advent of high-speed computers, this was considered infeasible due to the amount of work and time involved in hand-type calculations. Consequently, only recently have several authors[1,2,3,4,5] developed the theory and numerical techniques for calculating accurately lifting-surface effects.

This report presents a comparison of lifting-surface corrections calculated by two different numerical approaches for solution of the linear lifting-surface theory, i.e., the continuous distribution of vortices method[3,6,8] and the vortex-lattice method.[4,9,10] Also included for comparison purposes are those corrections based on a less rigorous approach.[7]

---

[1] References are listed on page 10 .

Calculations were made for a five-bladed free-running nonoptimum propeller and a four-bladed wake-adapted propeller. The third propeller of the comparison is identical to the wake-adapted propeller except that it is skewed.

SYNOPSIS OF THE PROPELLER LIFTING-SURFACE CALCULATIONS

The correction described in Reference 7 was based on calculations made by Ludweig and Ginzel.[11] Later, Ginzel[12,13] refined the theory. Ludweig and Ginzel related the flow curvature induced at the midchord to the downwash derivative. The downwash derivative, for constant circulation over the chord, is equal to the downwash produced by the vortex systems representing the blade outline. The result is a correction to camber. This camber correction, which relates the required camber in three-dimensional flow to the camber in the two-dimensional flow for the same coefficient of lift, depends primarily on blade shape, area, pitch, and radial circulation distribution.

In general, there still existed a deficiency in thrust for propellers designed by this method. Lerbs[14] felt that the deficiency was due to the limited solution for flow curvature, i.e., flow curvature induced over the entire chord was not defined. As a result of Lerbs' work, an additional pitch correction was derived but this correction sometimes resulted in overpitching of the propeller. Subsequent studies, however, have shown that this pitch correction is invalid when applied in addition to the camber correction.

An investigation by Cox[2] showed that Ginzel's calculations of the camber corrections were not correct. Errors in Ginzel's work were mainly due to the limited numerical accuracy obtained by the use of graphical methods in performing the calculations. Cox also showed the necessity of taking into account variations in blade shape and number.

Kerwin[4,9,10], in his vortex-lattice method, considers the solution of the lifting-surface problem for a propeller with arbitrary blade outline

and number of blades and constant pitch distribution for a uniform inflow velocity.

The method has recently been modified to account for a moderately varying pitch distribution and/or slightly nonuniform inflow velocities. The interval between the hub and tip of the blade is divided into several equal spaces, with half spaces at both ends. The radial strips are further divided in the chordwise direction into several spaces. Bound vortices are located at midpoints of each space and are connected at each end by a system of trailing vortices. The resulting network is called a vortex lattice. Strengths of the bound and trailing vortices are obtained from an assumed radial and chordwise circulation distribution. The total induced velocity induced at some point located at the midpoint of the lattice element can be found by summing the contributions of each lattice element. Camber and incidence corrections may then be found by comparing the induced camber lines with the corresponding results in two-dimensional flow for the same circulation distribution.

Kerwin found that the maximum camber computed for constant load propeller sections, for one control point located at the 3/4 chord, were in good agreement with results obtained for several points along the chord. The same agreement was noted by Sparenberg in Reference 1. For arbitrary loaded sections, however, at least three control points are needed.

The basic computer output from Kerwin's lifting-surface program is a radial distribution of camber correction factors, along with a distribution at the same radial points of pitch factors (see Table 1-a). The pitch factors, which is a correction to pitch due to effects of loading, is defined as the ratio of pitch correction (in radians) per unit lift coefficient. For cases of uniform loading and symmetrical blade outlines, no angular correction to pitch is present. The radial points at which the two corrections are computed depend upon the selection of the radial and chordwise lattice spacings.

In addition to the correction arising from loading, Kerwin[9] showed that the blade thickness induced a velocity in addition to those determined by the lifting-surface theory. As discussed previously, the blade loading

was represented by a vortex system located on the blades and in the wake behind each blade. Thickness on the other hand was represented by a distribution of sources and sinks whose strengths are proportional to the slope of the thickness form. The velocities induced are a function of the source and vortices distribution. In order to retain the specified loading, a correction to pitch due to thickness must be added. The thickness program of Kerwin gives a radial distribution of induced angles in degrees due to thickness (see Table 1-b) along with an additional correction to camber due to thickness.

Pien's[3,6,8] conditions for the lifting-surface model are similar to those of Kerwin's with the exception that Pien uses a continuous distribution of vortices. Consequently, Pien's approach is based on a more accurate procedure.? It makes use of the lifting-line model (through the point of reference) to avoid infinite integrals which considerably simplify the computation procedure.

The output from Pien's lifting-surface computer program presents for nine radii the chordwise distribution of camber and the chordwise distribution of the three-dimensional camber ratio (Table 2). Radial and chordwise output stations are the user's choice.

The radial distribution of incidence corrections to pitch due to loading is not specifically given in the computer output of Pien's lifting-surface program. The pitch correction, if any, will be automatically introduced when the meanline ordinates are plotted along the chord. For the purpose of making comparisons, the correction is obtained as follows: At each radius, the chordwise distribution of camber ratios are plotted and faired. The chordline of the faired profile is shifted such that it coincides with the fraction of chord-reference axis. The incidence correction to pitch is equal to the angular displacement of the profile chordline to the reference axis. An example of the procedure at several radii for the free-running propeller can be seen in Figure 2.

METHODS OF APPROACH

The lifting-line theory was used to determine the hydrodynamic pitch angle distribution (β_i), circulation distribuation (G), and the chord-length ratios (x/c) before the various lifting-surface corrections were applied.[15] In lifting-line theory, certain assumptions are made to reduce the difficult problem of flow distortion caused by the propeller as it rotates in the water. The propeller is assumed to be rotating at constant angular velocity and each blade is replaced by a lifting line whose circulation is a function of radial position. Variations in the circulation causes a free vortex surface, helical in shape, to be shed from the lifting line. The shape of the vortex sheet and velocity components induced in the flow by the propeller are mutually dependent; therefore, it is necessary to use an iterative procedure. Pitch of the propeller is determined by the angle of the resulting flow, including the induced velocities at the lifting line. For moderately-loaded propellers, the influence of the induced velocities on the downstream changes in shape of the vortex sheet is neglected. However, for heavily-loaded propellers, slipstream deformation must be taken into account.

The lifting-line theory describes the flow angularity but makes no attempt to define its curvature. Thus propellers designed by this method are underthrust unless supplemented by lifting-surface corrections.

As was previously stated, three propellers were designed by the methods given in References 3, 4, and 7. A five-bladed free-running propeller, a four-bladed wake-adapted propeller, and a four-bladed wake-adapted skewed propeller were designed. Two chordwise loadings, one similar to the NACA a = 1.0 meanline (constant chordwise loading) and one similar to the NACA a = 0.8 meanline were used. Drawings and pertinent data for each propeller model can be seen in Figures 1-a, b, and c.

RESULTS AND DISCUSSION

The results of the present work, comparing the lifting-surface corrections for the various numerical methods, are presented in tabular form (Tables 3 through 5), and graphical form (Figures 3 through 10). Figures 3 and 4 compare the radial distribution of the correction factors for camber. Kerwin's and Pien's results show large corrections at both the root and tip, while the results obtained by the design method of Reference 7 shows a constant correction near the outer region of the blade. The radial distribution of the corrected maximum camber ratios are compared in Figures 5 and 6. The results presented for Kerwin were computed from the relationship, that the corrected maximum camber is equal to the product of the camber correction factor and the uncorrected maximum camber. The shapes of the blade sections for both the skewed and nonskewed wake-adapted cases are the same. Thus the camber ratios are essentially the same. Figures 7 and 8 show the comparison of the chordwise distribution of camber ratios for the continuous distribution and vortex-lattice methods. Values shown for Pien's data are those values chosen after the correction was made in the manner shown in Figure 2. Kerwin's values were computed from the NACA camber to maximum camber ratio distribution for both $a = 1.0$ and $a = 0.8$ meanlines. Differences reflected in the maximum camber ratios between the two methods (Figures 5 and 6) are reflected in the chordwise distribution.

The continuous distribution program does not correct the pitch of the blade for changes in thickness. To make the pitch ratios of Figures 9 and 10 compatible, the thickness incidence correction computed by Kerwin's method was included in the final pitch ratios of the continuous distribution program. In comparing the two wake-adapted cases, i.e. with and without skew, the effects of skew produces higher pitch ratios than those obtained in the nonskewed case. Symmetry is lost with uniform loading which results in an incidence correction to pitch and an accompanying increase in pitch.

The pitch ratio results of Reference 7 are greater in all cases. This is partially due to Lerbs' additional correction to pitch which is used in

Reference 7. However, the results for both the vortex-lattice and continuous distribution methods, for cases of constant chordwise loading, are low due to the lack of any viscous correction. That is to say, the presence of a boundary layer affects the section's lift coefficient by distorting the pressure distribution. Fortunately, the theoretical lift for the a = 0.8 meanline compares very well with the experimental values.

Tables 3, 4, and 5 are tabulations of the camber correction factors, maximum camber ratios, and pitch ratios, respectively. The maximum camber ratios tabulated for Pien (Table 4) are the values obtained after the adjustment is made in the manner shown in Figure 2. The data is tabulated here for the reader's use. Table 6 compares the ratios of three-dimensional incidence correction to the two-dimensional corrections obtained by both numerical methods. The ratios are practically constant for results obtained from the Kerwin program. Also included in Table 6 is the radial distribution of incidence corrections due to thickness obtained by the Kerwin method.

From the theoretical standpoint, one would expect some differences between the two methods, especially for the skewed propeller. However, it is surprising to find that the results of the comparisons obtained by the vortex-lattice and the continuous distribution programs are fairly close. The discrepancies can be attributed to the different approaches between the two methods. Looking at the faired curves, as opposed to the symboled points for the lattice methods, one notices varying amounts of scatter, i.e., scatter for the free-running propeller far exceeds that of the two wake-adapted propellers. Figures 11-a and 11-b show the erratic nature of the lattice program as the radial and chordwise spacings are varied. The scatter collapses as the blade area ratio decreases, which probably accounts for the greater scatter with the free-running propeller (EAR = 1.2) than with the two wake-adapted propellers (EAR = 0.506).

As was previously stated, the vortex lattice size and shape is determined by the number and the distribution of radial and chordwise spacings about the control points. Convergence of the approximations and the accuracy of that convergence depend upon the lattice formed. However, the accuracy of this method, according to Schlichting and Thomas,[16] remains

unestablished* and is difficult to study theoretically.

Table 7 compares the circulation distribution computed by the lattice programs for the various spacings. The 16 radial and 16 chordwise spacings present values very close to those computed in Reference 7. However, in Figure 11, the corrections computed for this spacing are most erratic.

The calculated meanlines from the continuous distribution program at various radii for the three propellers are compared with the NACA meanlines in Table 8. Both the uniform and a = 0.8 chordwise loading distributions are presented. Values at the 0.5 and 0.6 radii compare favorably along the chord, while the root and tip distributions vary markedly. In all cases, the values presented show the sections are generally flatter in the regions near the nose and tail than for the two-dimensional sections. This is particularly true near the hub. The same results were noted by Lerbs.[17]

CONCLUSIONS

The comparisons made in this report are primarily to show the progress being made on lifting-surface corrections to lifting-line theory. Based on the results shown in the comparison, these few remarks are made:

1. The number of blades, blade shape and area, and blade loading are all important factors in determining the lifting-surface corrections.

2. The effects of blade thickness produces an additional correction to pitch and a negligible correction to camber.

---

* In Reference 10, the scatter is attributed to the manner in which the vortex-lattice spacing on the blade is arranged. The modified computer program with the arrangement of Reference 10 was not available at the time the calculations were made for this report.

3. For cases of asymmetrical chordwise load distribution, there is a large lifting-surface correction to the section ideal angle of attack.

4. The results show that the two-dimensional mean lines tend to be somewhat flatter at the leading and trailing edges as compared to the two-dimensional meanline (modified by the camber correction factor). Whether this difference is in any way due to the numerical procedures used is not known. It would appear that valid camber correction factors applied to two-dimensional meanline ordinates are, in general, reliable.

5. The method of Pien is preferable to that of Kerwin because the vortex-lattice concept is inaccurate for computations on the blade. The scatter is a consequence of this inaccurate model.

6. The lifting-surface corrections presented in Reference 7 should be superseded by the more rigorous lifting-surface calculations.

REFERENCES

1. Sparenberg, J. A., "Application of Lifting-Surface Theory of Ship Screws," International Shipbuilding Progress, Vol. 7, No. 67 (Mar 1960).

2. Cox, G. G., "Corrections to the Camber of Constant Pitch Propellers," Quarterly Transactions of the Royal Institution of Naval Architects, Vol. 103, pp. 227-243 (Jan 1961).

3. Pien, P. C., "The Calculation of Marine Propellers Based on Lifting Surface Theory," Journal of Ship Research, Vol. 5, No. 2, pp. 1-14 (Sep 1964).

4. Kerwin, J. E., "The Solution of Propeller Lifting-Surface Problems by the Vortex Lattice Methods," Department of Naval Architecture and Marine Engineering, Massachusetts Institute of Technology (Jun 1961).

5. Nelson, D. M., "A Lifting Surface Propeller Design Method for High-Speed Computers," NAVWEPS Report 9442 (Jan 1964).

6. Cheng, H. M., "Hydrodynamic Aspect of Propeller Design Based on Lifting-Surface Theory, Part I - Uniform Chordwise Load Distribution," David Taylor Model Basin Report 1802 (Sep 1964).

7. Morgan, W. B. and Eckhardt, M. K., "A Propeller Design Method," Transactions of the Society of Naval Architects and Marine Engineers, Vol. 63, pp. 325-374 (1955).

8. Cheng, H. M., "Hydrodynamic Aspect of Propeller Design Based on Lifting-Surface Theory, Part II - Arbitrary Chordwise Load Distribution," David Taylor Model Basin Report 1803 (Jun 1965).

9. Kerwin, J. E. and Leopold, R., "Propeller Incidence Correction Due to Blade Thickness," Journal of Ship Research, Vol. 7, No. 2, pp. 1-6 (Oct 1963).

10. Kerwin, J. E. and Leopold, R., "A Design Theory for Subcavitating Propellers," The Society of Naval Architects and Marine Engineers," Vol. 72 (Nov 1964).

11. Ludweig, H. and Ginzel, I., "On the Theory of Screws with Wide Blades," Aerodynamische Versuchsanstalt, Goettingen Report 44/A/09 (1944).

12. Ginzel, J. I., "Influence of Blade Shape and of Circulation Distribution on the Camber Correction Factor," Admiralty Research Laboratory Report ARL/R2/HY/7/1 (Oct 1951).

13. Ginzel, J. I., "Theory of the Broad Bladed Propeller," Admiralty Research Laboratory Report ARL/R3/HY/7/1 (Jun 1952).

14. Lerbs, H. W., "Propeller Pitch Correction Arising from Lifting Surface Effects," David Taylor Model Basin Report 942 (Feb 1955).

15. Hecker, R., "Manual for Preparing and Interpreting Data of High-Speed Computers at the David Taylor Model Basin," David Taylor Model Basin Report 1244 (Aug 1959).

16. Schlichting, H. and Thomas, H. H. B. M., "Note on the Calculation of the Lift Distribution of Swept Wings," Rep. Aero. Res. Coun., London 11300 (1947).

17. Lerbs, H. W. et al, "Numerische Auswertungen zue Theorie der Tragenden Flache von Propellern," Schiffbautechnische Gesellschaft, Band 58 (1964).

RADIUS		PITCH FACTOR		CAMBER FACTOR		PITCH FACTOR		CAMBER FACTOR
0.375	A = .8 mean line	0.057		2.103	A = 1.0 mean line	0.000		2.418
0.475		0.059		1.979		0.000		2.251
0.575		0.060		1.793		0.000		1.989
0.675		0.054		1.807		0.000		1.981
0.775		0.053		1.587		0.000		1.656
0.875		0.046		2.070		0.000		2.236

(a) - Lifting Surface Program

R	$(\alpha_t)_{ALPHA}$	CO
0.25	1.056	0.001
0.35	0.935	0.001
0.45	0.788	0.000
0.55	0.649	0.000
0.65	0.519	0.000
0.75	0.389	0.000
0.85	0.264	0.000
0.95	0.190	0.000

(b) - Thickness Program

Table 1 - Sample Computer Output from Kerwin's Lifting Surface and Thickness Programs (for the Free Running Propeller).

RX/RU	0.2500	0.3000	0.4000	0.5000	0.6000	0.7000	0.8000	0.9000	0.9500
CAMBER DISTRIBUTION FREE RUNNING PROPELLER A=.8 MEAN LINE									
X/ℓ									
0.0100	0.0048	0.0064	0.0069	0.0056	0.0048	0.0042	0.0032	0.0030	0.0010
0.1000	0.0392	0.0492	0.0456	0.0421	0.0350	0.0302	0.0230	0.0186	0.0127
0.2000	0.0656	0.0794	0.0728	0.0659	0.0532	0.0466	0.0343	0.0281	0.0143
0.3500	0.0880	0.1050	0.0939	0.0836	0.0655	0.0581	0.0406	0.0303	0.0064
0.5000	0.0908	0.1077	0.0942	0.0828	0.0645	0.0578	0.0398	0.0253	0.0065
0.6500	0.0746	0.0872	0.0747	0.0646	0.0502	0.0457	0.0310	0.0192	0.0043
0.8000	0.0380	0.0412	0.0308	0.0236	0.0155	0.0163	0.0078	-0.0015	-0.0083
0.9000	0.0029	-0.0062	-0.0170	-0.0219	-0.0228	-0.0127	-0.0140	-0.0183	-0.0173
0.9900	-0.0321	-0.0555	-0.0674	-0.0705	-0.0627	-0.0408	-0.0336	-0.0285	-0.0235
CAMBER RATIO									
X/ℓ									
0.0100	0.0012	0.0014	0.0011	0.0009	0.0008	0.0007	0.0006	0.0009	0.0007
0.1000	0.0102	0.0110	0.0086	0.0072	0.0057	0.0053	0.0046	0.0058	0.0087
0.2000	0.0170	0.0177	0.0138	0.0112	0.0087	0.0082	0.0069	0.0088	0.0098
0.3500	0.0229	0.0234	0.0178	0.0142	0.0107	0.0103	0.0082	0.0095	0.0044
0.5000	0.0236	0.0240	0.0178	0.0141	0.0106	0.0102	0.0080	0.0079	0.0045
0.6500	0.0194	0.0194	0.0142	0.0110	0.0082	0.0081	0.0063	0.0060	0.0029
0.8000	0.0099	0.0092	0.0058	0.0040	0.0025	0.0029	0.0016	-0.0005	-0.0057
0.9000	0.0007	-0.0014	-0.0032	-0.0037	-0.0037	-0.0022	-0.0028	-0.0057	-0.0119
0.9900	-0.0083	-0.0124	-0.0128	-0.0120	-0.0103	-0.0072	-0.0068	-0.0089	-0.0161

CAMBER DISTRIBUTION FREE RUNNING PROPELLER A=1.0 MEAN LINE									
X/ℓ									
0.0100	0.0047	0.0060	0.0058	0.0056	0.0048	0.0041	0.0031	0.0028	0.0013
0.1000	0.0393	0.0494	0.0451	0.0435	0.0361	0.0303	0.0226	0.0190	0.0109
0.2000	0.0670	0.0812	0.0763	0.0705	0.0569	0.0479	0.0345	0.0275	0.0163
0.3500	0.0930	0.1121	0.1036	0.0942	0.0744	0.0627	0.0433	0.0310	0.0185
0.5000	0.1016	0.1224	0.1123	0.1015	0.0796	0.0671	0.0459	0.0286	0.0190
0.6500	0.0930	0.1121	0.1036	0.0942	0.0744	0.0627	0.0433	0.0310	0.0185
0.8000	0.0670	0.0812	0.0763	0.0705	0.0569	0.0479	0.0345	0.0275	0.0163
0.9000	0.0393	0.0494	0.0451	0.0435	0.0361	0.0303	0.0226	0.0190	0.0109
0.9900	0.0047	0.0060	0.0058	0.0056	0.0048	0.0041	0.0031	0.0028	0.0013
CAMBER RATIO									
X/ℓ									
0.0100	0.0012	0.0013	0.0011	0.0010	0.0008	0.0007	0.0006	0.0009	0.0009
0.1000	0.0102	0.0108	0.0087	0.0074	0.0059	0.0053	0.0046	0.0056	0.0075
0.2000	0.0174	0.0181	0.0145	0.0120	0.0093	0.0085	0.0070	0.0086	0.0112
0.3500	0.0242	0.0250	0.0196	0.0160	0.0122	0.0111	0.0087	0.0097	0.0127
0.5000	0.0264	0.0273	0.0213	0.0173	0.0131	0.0118	0.0092	0.0089	0.0130
0.6500	0.0242	0.0250	0.0196	0.0160	0.0122	0.0111	0.0087	0.0097	0.0127
0.8000	0.0174	0.0181	0.0145	0.0120	0.0093	0.0085	0.0070	0.0086	0.0112
0.9000	0.0102	0.0108	0.0087	0.0074	0.0059	0.0053	0.0046	0.0056	0.0075
0.9900	0.0012	0.0013	0.0011	0.0010	0.0008	0.0007	0.0006	0.0009	0.0009

Table 2 - Sample Output from Pien's Lifting Surface Program (for the Free Running Propeller).

Free Running

r/R	A = 0.8			A = 1.0		
	$\frac{M_{x_3}}{M_{x_2}}$ (P)	$\frac{M_{x_3}}{M_{x_2}}$ (K)	$\frac{M_{x_3}}{M_{x_2}}$ Ref. 7	$\frac{M_{x_3}}{M_{x_2}}$ (P)	$\frac{M_{x_3}}{M_{x_2}}$ (K)	$\frac{M_{x_3}}{M_{x_2}}$ Ref. 7
200			1.0400			1.0400
.250	2.2284			2.6238		
.300	2.4141	2.2860	1.2595	2.6538	2.6510	1.2595
.325		2.2180			2.6610	
.350		2.0870			2.4050	
.375		2.1030			2.4180	
.400	1.9683	1.9750	1.5036	2 1078	2 2640	1.5036
.425		1 9825			1.3990	
.433		2 0470			2.3400	
.450		1.9770			2.2550	
.475		1.9790			2.2510	
.480		1.9400			2.2050	
.500	1.8899	1.8220	1.7373	1.9213	2.0700	1.7373
.525		1.8335			2.0195	
.550		1.8000			2.0050	
.560		1.8080			2.0160	
.567		1.8080			2.0290	
.575		1.7930			1.9890	
.600	1.7692		1.9895	1.8108		1.9895
.625		1.6480			1.8840	
.633		1.8460			2.0540	
.640		1.7310			1.8920	
.650		1.7060			1.8540	
.675		1.8070			1.9810	
.700	1.6750	1.8020	2.2278	1.8154	1.9670	2.2278
.720		1.8210			1.9850	
.725		1.7325			1.9400	
.750		1.6960			1.8090	
.775		1.5870			1.6560	
.800	1.6956	1.7040	2.4194	1.6964	1.7790	2.4194
.825		1.7490			1.7770	
.833		1.6460			1.6820	
.850		1.8650			1.9950	
.875		2.0700			2.2360	
.900	2.0000	2.5424	2.5424	1.7500		2.5424
.950	2.4118			2.3750		

TABLE 3a

Values of Camber Corrections $\left(\frac{M_{x_3}}{M_{x_2}}\right)$ at Various Nondimensional Radii $\left(\frac{r}{R}\right)$

Wake Adapted without Skew

r/R	A = 0.8			A = 1.0		
	$\frac{M_{x3}}{M_{x2}}$ (P)	$\frac{M_{x3}}{M_{x2}}$ (K)	$\frac{M_{x3}}{M_{x2}}$ Ref. 7	$\frac{M_{x3}}{M_{x2}}$ (P)	$\frac{M_{x3}}{M_{x2}}$ (K)	$\frac{M_{x3}}{M_{x2}}$ Ref. 7
.200			.9200			.9200
.225						
.250	1.1880			1.2210		
.275						
.300	1.4064		1.0530	1.4970		1.0530
.325		1.2800			1.3420	
.350		1.1860			1.1970	
.375		1.2170			1.2330	
.400	1.1345		1.2390	1.1810		1.2390
.425		1.1820			1.2200	
.450		1.1730			1.1780	
.475		1.2010			1.2120	
.500	1.1420		1.4490	1.1990		1.4490
.525		1.2020			1.2430	
.550		1.2050			1.2160	
.575		1.2350			1.2540	
.600	1.1719		1.6370	1.2330		1.6370
.625		1.2590			1.3130	
.650		1.2640			1.2880	
.675		1.2880			1.3180	
.700	1.2070		1.7760	1.2650		1.7760
.725		1.3630			1.4390	
.750		1.3460			1.3870	
.775		1.4200			1.4820	
.800	1.3579		1.8280	1.4730		1.8280
.825		1.4900			1.5990	
.850		1.5640			1.6710	
.875		1.6050			1.7060	
.900	1.6580		1.8320	1.8090		1.8320
.925						
.950	1.6817			1.7710		

TABLE 3b

Values of Camber Corrections $\left(\frac{M_{x3}}{M_{x2}}\right)$ at Various Nondimensional Radii $\left(\frac{r}{R}\right)$

Wake Adapted with Skew

r/R	A = 0.8			A = 1.0		
	$\frac{M_{x3}}{M_{x2}}$ (P)	$\frac{M_{x3}}{M_{x2}}$ (K)	$\frac{M_{x3}}{M_{x2}}$ Ref. 7	$\frac{M_{x3}}{M_{x2}}$ (P)	$\frac{M_{x3}}{M_{x2}}$ (K)	$\frac{M_{x3}}{M_{x2}}$ Ref. 7
.200			.9200			.9200
.225						
.250	1.1150			1.1150		
.275						
.300	1.4064		1.0530	1.4850		1.0530
.325		1.2740			1.3480	
.350		1.1800			1.2050	
.375		1.2120			1.2420	
.400	1.1100		1.2390	1.1810		1.2390
.425		1.1990			1.2590	
.450		1.1750			1.2030	
.475		1.1940			1.2270	
.500	1.1030		1.4490	1.2040		1.4490
.525		1.1830			1.2440	
.550		1.2060			1.2430	
.575		1.2330			1.2760	
.600	1.1540		1.6370	1.2380		1.6370
.625		1.2640			1.3410	
.650		1.2880			1.3460	
.675		1.2870			1.3470	
.700	1.2120		1.7760	1.3160		1.7760
.725		1.3640			1.4720	
.750		1.4020			1.4900	
.775		1.4410			1.5360	
.800	1.3520		1.8280	1.4800		1.8280
.825		1.5670			1.7150	
.850		1.6400			1.7780	
.875		1.7210			1.8780	
.900	1.6500		1.8320	1.7930		1.8320
.925						
.950	1.7790			1.9680		

TABLE 3c

Values of Camber Corrections $\left(\frac{M_{x3}}{M_{x2}}\right)$ at Various Nondimensional Radii $\left(\frac{r}{R}\right)$

Free Running

r/R	A = 0.8			A = 1.0		
	$M_x/\ell_{(P)}$	$M_x/\ell_{(K)}$	M_x/ℓ Ref. 7	$M_x/\ell_{(P)}$	$M_x/\ell_{(K)}$	M_x/ℓ Ref. 7
.200			.0156			.0127
.250	.0293			.0265		
.300	.0309	.0293	.0199	.0276	.0276	.0162
.325		.0286			.0279	
.350		.0267			.0255	
.375		.0265			.0247	
.400	.0248	.0249	.0212	.0215	.0232	.0172
.425		.0242			.0235	
.433		.0247			.0229	
.450		.0233			.0216	
.475		.0225			.0209	
.480		.0219			.0203	
.500	.0206	.0199	.0205	.0171	.0183	.0167
.525		.0192			.0170	
.550		.0178			.0160	
.560		.0176			.0157	
.567		.0174			.0157	
.575		.0170			.0145	
.600	.0161		.0186	.0134		.0151
.625		.0145			.0134	
.633		.0159			.0144	
.640		.0147			.0130	
.650		.0143			.0126	
.675		.0148			.0131	
.700	.0134	.0144	.0176	.0118	.0128	.0143
.720		.0140			.0123	
.725		.0132			.0120	
.750		.0126			.0109	
.775		.0116			.0096	
.800	.0117	.0118	.0150	.0095	.0099	.0122
.825		.0121			.0099	
.833		.0113			.0092	
.850		.0127			.0095	
.875		.0141			.0123	
.900	.0138		.0150	.0098		.0122
.950	.0126			.0133		

TABLE 4a

.Values of the Maximum Camber Ratios $\left(\frac{M_{x_3}}{\ell}\right)$ at Various Nondimensional Radii $\left(\frac{r}{R}\right)$

Wake Adapted without Skew

r/R	A = 0.8			A = 1.0		
	$M_x/\ell_{(P)}$	$M_x/\ell_{(K)}$	M_x/ℓ Ref. 7	$M_x/\ell_{(P)}$	$M_x/\ell_{(K)}$	M_x/ℓ Ref. 7
.200			.0349			.0284
.225						
.250	.0374			.0312		
.275						
.300	.0435		.0360	.0376		.0292
.325		.0391			.0333	
.350		.0357			.0293	
.375		.0360			.0297	
.400	.0329		.0367	.0278		.0298
.425		.0335			.0280	
.450		.0323			.0263	
.475		.0320			.0262	
.500	.0292		.0370	.0249		.0300
.525		.0297			.0249	
.550		.0287			.0235	
.575		.0284			.0234	
.600	.0261		.0363	.0223		.0294
.625		.0270			.0229	
.650		.0263			.0217	
.675		.0259			.0215	
.700	.0235		.0345	.0200		.0280
.725		.0257			.0211	
.750		.0247			.0207	
.775		.0252			.0214	
.800	.0236		.0320	.0208		.0260
.825		.0250			.0218	
.850		.0255			.0221	
.875		.0253			.0219	
.900	.0254		.0291	.0225		.0236
.925						
.950	.0242			.0207		

TABLE 4b

Values of the Maximum Camber Ratios $\left(\frac{M_{x_3}}{\ell}\right)$ at Various Nondimensional Radii $\left(\frac{r}{R}\right)$

Wake Adapted with Skew

r/R	A = 0.8			A = 1.0		
	$M_x/\ell_{(P)}$	$M_x/\ell_{(K)}$	M_x/ℓ Ref. 7	$M_x/\ell_{(P)}$	$M_x/\ell_{(K)}$	M_x/ℓ Ref. 7
.200			.0349			.0284
.225						
.250	.0351			.0285		
.275						
.300	.0435		.0360	.0373		.0292
.325		.0390			.0335	
.350		.0356			.0295	
.375		.0359			.0299	
.400	.0322		.0367	.0278		.0298
.425		.0339			.0289	
.450		.0324			.0269	
.475		.0318			.0265	
.500	.0282		.0370	.0250		.0300
.525		.0292			.0250	
.550		.0287			.0241	
.575		.0283			.0238	
.600	.0257		.0363	.0224		.0294
.625		.0271			.0234	
.650		.0268			.0227	
.675		.0259			.0220	
.700	.0236		.0345	.0208		.0280
.725		.0258			.0226	
.750		.0257			.0222	
.775		.0256			.0222	
.800	.0235		.0320	.0209		.0260
.825		.0263			.0234	
.850		.0267			.0235	
.875		.0272			.0241	
.900	.0254		.0291	.0223		.0236
.925						
.950	.0256			.0230		

TABLE 4c

Values of the Maximum Camber Ratios $\left(\frac{M_{x_3}}{\ell}\right)$ at Various Nondimensional Radii $\left(\frac{r}{R}\right)$

Free Running

r/R	A = 0.8			A = 1.0		
	$P/D_{(P)}$	$P/D_{(K)}$	$P/D_{Ref.\ 7}$	$P/D_{(P)}$	$P/D_{(K)}$	$P/D_{Ref.\ 7}$
.200			1.3170			1.3393
.250	1.3091			1.2822		
.300	1.3332	1.3239	1.3120	1.2971	1.2947	1.3321
.325		1.3172			1.2915	
.350		1.3134			1.2865	
.375		1.3106			1.2838	
.400	1.3103	1.2998	1.2970	1.2756	1.2736	1.3170
.425		1.2956			1.2712	
.433		1.2930			1.2666	
.450		1.3003			1.2738	
.475		1.2842			1.2568	
.480		1.2777			1.2526	
.500	1.2794	1.2687	1.2730	1.2443	1.2463	1.2901
.525		1.2568			1.2360	
.550		1.2474			1.2248	
.560		1.2472			1.2249	
.567		1.2430			1.2217	
.575		1.2442			1.2202	
.600	1.2420		1.2420	1.2146		1.2565
.625		1.2223			1.2039	
.633		1.2187			1.1987	
.640		1.2172			1.1972	
.650		1.2121			1.1927	
.675		1.2039			1.1855	
.700	1.1968	1.1913	1.2050	1.1722	1.1736	1.2195
.720		1.1900			1.1725	
.725		1.1816			1.1668	
.750		1.1741			1.1578	
.775		1.1671			1.1503	
.800	1.1538	1.1513	1.1620	1.1338	1.1348	1.1830
.825		1.1472			1.1329	
.833		1.1178			1.1012	
.850		1.1349			1.1201	
.875		1.1286			1.1137	
.900	1.1225		1.1310	1.1001		1.1466
.950	1.1180			1.0647		

TABLE 5a

Values of the Pitch Ratio $\left(\frac{P}{D}\right)$ at Various Nondimensional Radii $\left(\frac{r}{R}\right)$

Wake Adapted without Skew

r/R	A = 0.8			A = 1.0		
	$P/D_{(P)}$	$P/D_{(K)}$	$P/D_{\text{Ref. 7}}$	$P/D_{(P)}$	$P/D_{(K)}$	$P/D_{\text{Ref. 7}}$
.200			.9800			1.0157
.225						
.250	1.0139			.9628		
.275						
.300	1.0326		1.0410	.9857		1.0744
.325		1.0333			.9972	
.350		1.0399			1.0035	
.375		1.0478			1.0115	
.400	1.0570		1.0810	1.0167		1.1143
.425		1.0536			1.0205	
.450		1.0627			1.0290	
.475		1.0685			1.0352	
.500	1.0715		1.1110	1.0365		1.1422
.525		1.0750			1.0445	
.550		1.0837			1.0519	
.575		1.0854			1.0541	
.600	1.0823		1.1290	1.0482		1.1589
.625		1.0851			1.0553	
.650		1.0832			1.0530	
.675		1.0823			1.0517	
.700	1.0929		1.1430	1.0583		1.1726
.725		1.0880			1.0586	
.750		1.0918			1.0610	
.775		1.0998			1.0685	
.800	1.0988		1.1540	1.0669		1.1848
.825		1.0984			1.0683	
.850		1.0896			1.0598	
.875		1.0948			1.0631	
.900	1.1077		1.1620	1.0736		1.1897
.925						
.950	1.1185			1.0819		

TABLE 5b

Values of the Pitch Ratio $\left(\frac{P}{D}\right)$ at Various Nondimensional Radii $\left(\frac{r}{R}\right)$

Wake Adapted with Skew

r/R	A = 0.8			A = 1.0		
	$P/D_{(P)}$	$P/D_{(K)}$	$P/D_{Ref.\ 7}$	$P/D_{(P)}$	$P/D_{(K)}$	$P/D_{Ref.\ 7}$
.200			.9800			1.0157
.225						
.250	1.0250			.9716		
.275						
.300	1.0331		1.0410	.9876		1.0744
.325		1.0559			1.0176	
.350		1.0623			1.0243	
.375		1.0720			1.0341	
.400	1.0665		1.0810	1.0298		1.1143
.425		1.0782			1.0436	
.450		1.0908			1.0556	
.475		1.0998			1.0641	
.500	1.0854		1.1110	1.0558		1.1422
.525		1.1078			1.0759	
.550		1.1110			1.0778	
.575		1.1106			1.0780	
.600	1.0934		1.1290	1.0637		1.1589
.625		1.1055			1.0754	
.650		1.1057			1.0744	
.675		1.1094			1.0776	
.700	1.0981		1.1430	1.0681		1.1726
.725		1.1114			1.0803	
.750		1.1081			1.0771	
.775		1.1114			1.0822	
.800	1.0964		1.1540	1.0669		1.1848
.825		1.0969			1.0758	
.850		1.0747			1.0465	
.875		1.0815			1.0513	
.900	1.0878		1.1620	1.0526		1.1897
.925						
.950	1.0951			1.0400		

TABLE 5c

Values of the Pitch Ratio $\left(\frac{P}{D}\right)$ at Various Nondimensional Radii $\left(\frac{r}{R}\right)$

r/R	Free Running Propeller			Wake Adapted Non-Skewed			Wake Adapted Skewed		
	$\frac{\alpha_{i3D}}{\alpha_{i2D}}_{(K)}$	$\frac{\alpha_{i3D}}{\alpha_{i2D}}_{(P)}$	$\alpha_{t_{(K)}}$	$\frac{\alpha_{i3D}}{\alpha_{i2D}}_{(K)}$	$\frac{\alpha_{i3D}}{\alpha_{i2D}}_{(P)}$	$\alpha_{t_{(K)}}$	$\frac{\alpha_{i3D}}{\alpha_{i2D}}_{(K)}$	$\frac{\alpha_{i3D}}{\alpha_{i2D}}_{(P)}$	$\alpha_{t_{(K)}}$
.250		1.858	1.056		1.772	1.265		2.447	**1.265**
.300		2.697			1.895			1.912	
.325	2.083			1.488			2.381		
.350	2.008		0.935	1.491		0.973	2.386		**0.973**
.375	2.120			1.488			2.456		
.400		2.830			1.663			2.047	
.425	2.158			1.376			2.381		
.450	2.158		0.788	1.413		0.675	2.566		**0.675**
.475	2.195			1.413			2.715		
.500		3.013			1.521			2.114	
.525	2.195			1.339			2.752		
.550	2.195		0.649	1.413		0.451	2.605		**0.451**
.575	2.232			1.413			2.530		
.600		3.035			1.530			2.031	
.625	2.195			1.377			2.307		
.650	2.083		0.519	1.413		0.301	2.456		**0.301**
.675	2.008			1.451			2.716		
.700		2.498			1.644			1.894	
.725	1.972			1.413			2.530		
.750	1.897		0.389	1.488		0.204	2.269		**0.204**
.775	1.972			1.525			2.195		
.800		2.721			1.555			1.438	
.825	2.008			1.488			1.414		
.850	1.711		0.264	1.488		0.142	0.744		0.142
.875	1.711			1.599			0.930		
.900		3.501			1.733			0.725	
.950		3.501	0.190		1.887	0.128		0.680	0.128

TABLE 6

Values of the Incidence Correction Ratios $\left(\frac{\alpha_{i3D}}{\alpha_{i2D}}\right)$ due to Camber and Incidence Correction (α_t) due to Thickness at Various Nondimensional Radii (r/R)

r/R	$G = \Gamma/2\pi RV_a$			
	LERBS	KERWIN		
		i	ii	iii
.2	0.0	0.0	0.0	0.0
.3	0.015295	0.0152	0.0156	0.0165
.4	0.020720	0.0208	0.0209	0.0213
.5	0.023243	0.0232	0.0234	0.0235
.6	0.023317	0.0232	0.0234	0.0235
.7	0.021491	0.0214	0.0215	0.0217
.8	0.018133	0.0181	0.0180	0.0185
.9	0.012954	0.0130	0.0128	0.0138
1.0	0.0	0.0	0.0	0.0

Lattice Spacing		
i	16 Radial	16 Chordwise
ii	16 Radial	8 Chordwise
iii	8 Radial	8 Chordwise

TABLE 7

Comparison of Circulation Distributions (G) Computed by the Vortex Lattice Method and by Induction Factors

Free Running

	x/c	M/M_x*	.25	.3	.4	.5	.6	.7	.8	.9	.95
A = .8	.01	.073	.0459	.0485	.0484	.0485	.0497	.0493	.0598	.0424	.0427
	.10	.448	.3922	.4013	.4032	.4126	.4224	.4223	.4530	.5072	.6463
	.20	.699	.6679	.6602	.6694	.6699	.6770	.6901	.7180	.7319	.7927
	.35	.920	.9258	.9126	.9153	.9126	.9130	.9225	.9231	.9783	.9756
	.50	1.000	1.0000	1.0000	1.0000	1.0000	1.0000	1.0000	1.0000	1.0000	1.0000
	.65	.943	.9011	.9158	.9436	.9466	.9565	.9296	.9487	.9855	.8537
	.80	.703	.6149	.6505	.6895	.6990	.7019	.6478	.6410	.6449	.5671
	.90	.359	.3251	.3527	.3831	.3884	.3851	.3457	.3333	.3482	.3000
	.99	.027	.0353	.0388	.0484	.0388	.0373	.0423	.0427	.0362	.0305
A = 1.0	.01	.073	.0455	.0476	.0516	.0578	.0763	.0847	.1087	.0732	.0692
	.10	.469	.3864	.3956	.4085	.4277	.4504	.4492	.4999	.4553	.5769
	.20	.722	.6591	.6630	.6808	.6936	.7099	.7203	.7609	.6992	.8615
	.35	.935	.9167	.9158	.9202	.9249	.9313	.9407	.9457	.9106	.9769
	.50	1.000	1.0000	1.0000	1.0000	1.0000	1.0000	1.0000	1.0000	1.0000	1.0000
	.65	.935	.9167	.9158	.9202	.9249	.9313	.9407	.9457	.9106	.9769
	.80	.722	.6591	.6630	.6808	.6936	.7099	.7203	.7609	.6992	.8615
	.90	.469	.3864	.3956	.4085	.4277	.4504	.4492	.4999	.4553	.5769
	.99	.073	.0455	.0476	.0516	.0578	.0763	.0847	.1087	.0732	.0692

*Two dimensional. NACA

TABLE 8a

Comparison of the Calculated Mean Line Distribution at VariousNondimensional Radii with the NACA Mean Line Distribution

Wake Adapted without Skew

	x/c	M/M_x*	.25	.3	.4	.5	.6	.7	.8	.9	.95
A = .6	.01	.073	.0609	.0585	.0612	.0641	.0628	.0600	.0577	.0578	.0580
	.10	.448	.4487	.4388	.4604	.4567	.4529	.4550	.4423	.4444	.5121
	.20	.699	.7083	.6995	.7158	.7131	.7130	.7100	.7019	.7067	.7633
	.35	.920	.9295	.9282	.9317	.9317	.9327	.9300	.9279	.9289	.9227
	.50	1.000	1.0000	1.0000	1.0000	1.0000	1.0000	1.0000	1.0000	1.0000	1.0000
	.65	.943	.9295	.9282	.9317	.9317	.9327	.9300	.9279	.9289	.9227
	.80	.703	.7083	.6995	.7158	.7131	.7130	.7100	.7019	.7067	.7633
	.90	.359	.4487	.4388	.4604	.4567	.4529	.4550	.4423	.4444	.5121
	.99	.027	.0609	.0585	.0612	.0641	.0628	.0600	.0577	.0578	.0580
A = 1.0	.01	.073	.0562	.0529	.0578	.0616	.0575	.0553	.0551	.0551	.0579
	.10	.469	.4251	.4230	.4347	.4349	.4330	.4340	.4280	.4291	.4793
	.20	.722	.6792	.6805	.6869	.6884	.6858	.6809	.6822	.6850	.7355
	.35	.935	.9118	.9172	.9149	.9144	.9119	.9106	.9153	.9173	.8967
	.50	1.000	1.0000	1.0000	1.0000	1.0000	1.0000	1.0000	1.0000	1.0000	1.0000
	.65	.935	.9420	.9402	.9453	.9384	.9367	.9464	.9280	.9213	.9380
	.80	.722	.7059	.6920	.7021	.6884	.6858	.6766	.6610	.6260	.5620
	.90	.469	.3877	.3770	.3799	.3733	.3717	.3575	.3432	.3189	.2562
	.99	.073	.0348	.0368	.0365	.0342	.0385	.0340	.0339	.0315	.0289

*Two dimensional. NACA

TABLE 8b

Comparison of the Calculated Mean Line Distribution at Various Nondimensional Radii with the NACA Mean Line Distribution

Wake Adapted with Skew

	x/c	M/M_x*	.25	.3	.4	.5	.6	.7	.8	.9	.95
A = .8	.01	.073	.0598	.0552	.0590	.0603	.0623	.0593	.0596	.0630	.0586
	.10	.448	.4758	.4230	.4441	.4539	.4553	.4619	.4468	.4370	.4570
	.20	.699	.7493	.6782	.6988	.7128	.7082	.7161	.7021	.6890	.7461
	.35	.920	.9430	.9149	.9255	.9326	.9300	.9322	.9319	.9252	.9453
	.50	1.000	1.0000	1.0000	1.0000	1.0000	1.0000	1.0000	1.0000	1.0000	1.0000
	.65	.943	.9601	.9356	.9379	.9291	.9261	.9195	.9234	.9291	.9258
	.80	.703	.7293	.6943	.6863	.6809	.6771	.6653	.6723	.6614	.5977
	.90	.359	.4046	.3793	.4006	.3653	.4942	.3559	.3660	.3543	.3008
	.99	.027	.0427	.0414	.0280	.0221	.0428	.0339	.0426	.0472	.0391
A = 1.0	.01	.073	.0596	.0590	.0647	.0640	.0670	.0625	.0622	.0628	.0609
	.10	.469	.5123	.4424	.4640	.4720	.4732	.4760	.4593	.4574	.4739
	.20	.722	.7965	.7051	.7590	.7280	.7321	.7356	.7177	.7130	.7565
	.35	.935	.9719	.9330	.9389	.9400	.9464	.9471	.9426	.9417	.9565
	.50	1.000	1.0000	1.0000	1.0000	1.0000	1.0000	1.0000	1.0000	1.0000	1.0000
	.65	.935	.9368	.9223	.9281	.9280	.9196	.9135	.9187	.9238	.9130
	.80	.722	.7158	.6917	.7050	.7120	.6920	.6875	.6938	.6816	.6783
	.90	.469	.4561	.4290	.4532	.4640	.4375	.4327	.4354	.4215	.3652
	.99	.073	.0526	.0429	.0575	.0800	.0536	.0577	.0670	.0628	.0348

*Two dimensional. NACA

TABLE 8c

Comparison of the Calculated Mean Line Distribution at Various Nondimensional Radii with the NACA Mean Line Distribution

NUMBER OF BLADES: Z = 5.0 DIAMETER: D = 12.5'

EXPANDED AREA RATIO: EAR = 0.960 ROTATION: RH

MEAN LINE TYPE: A = 0.800 BLADE OUTLINE: SYMMETRICAL

PITCH DISTRIBUTION: NON-OPTIMUM

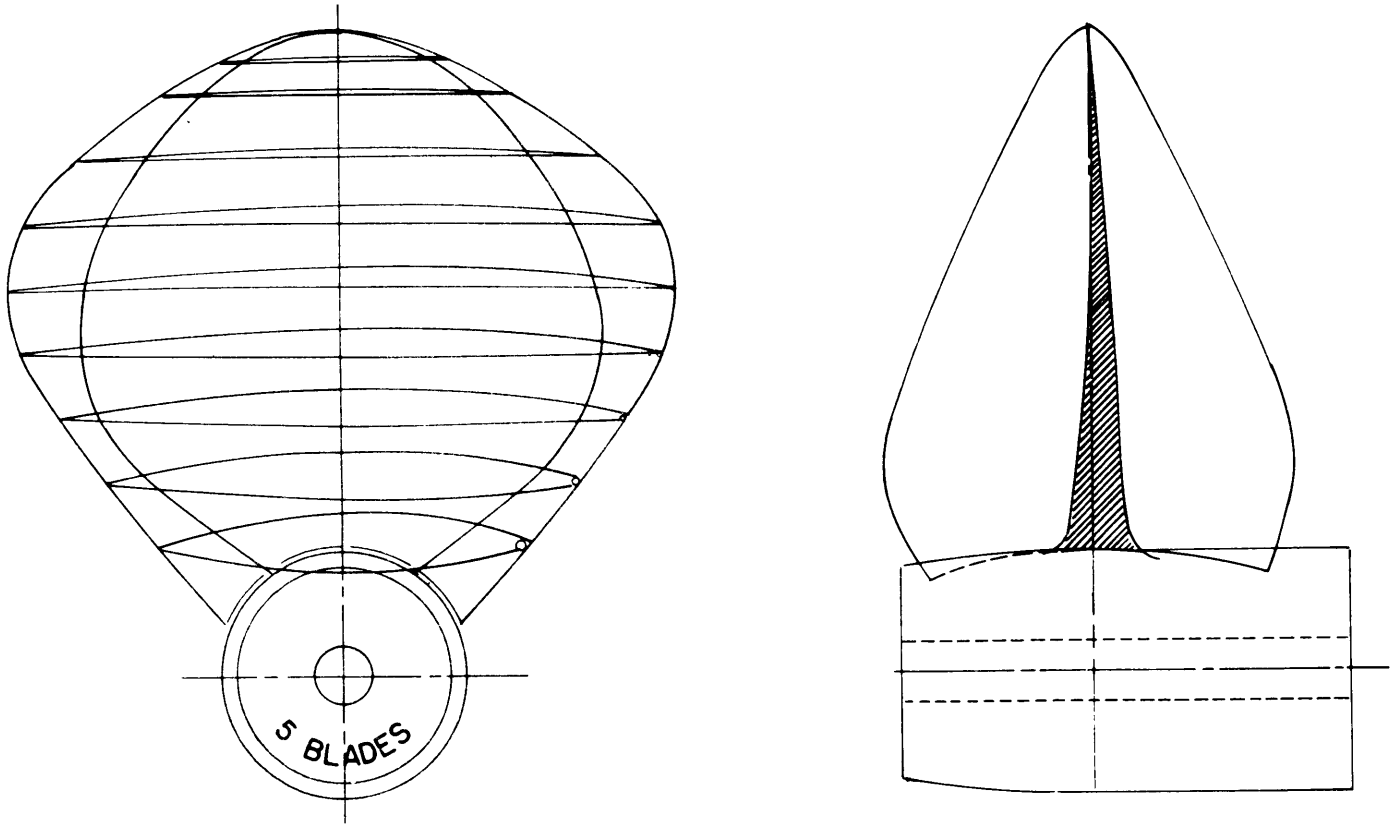

Figure 1 (a) - Drawing of the Free Running Propeller

NUMBER OF BLADES: Z = 4.0 DIAMETER: D = 21.0'

EXPANDED AREA RATIO: EAR = 0.506 ROTATION: RH

MEAN LINE TYPE: A = 0.800 BLADE OUTLINE: SYMMETRICAL

PITCH DISTRIBUTION: LERBS OPTIMUM

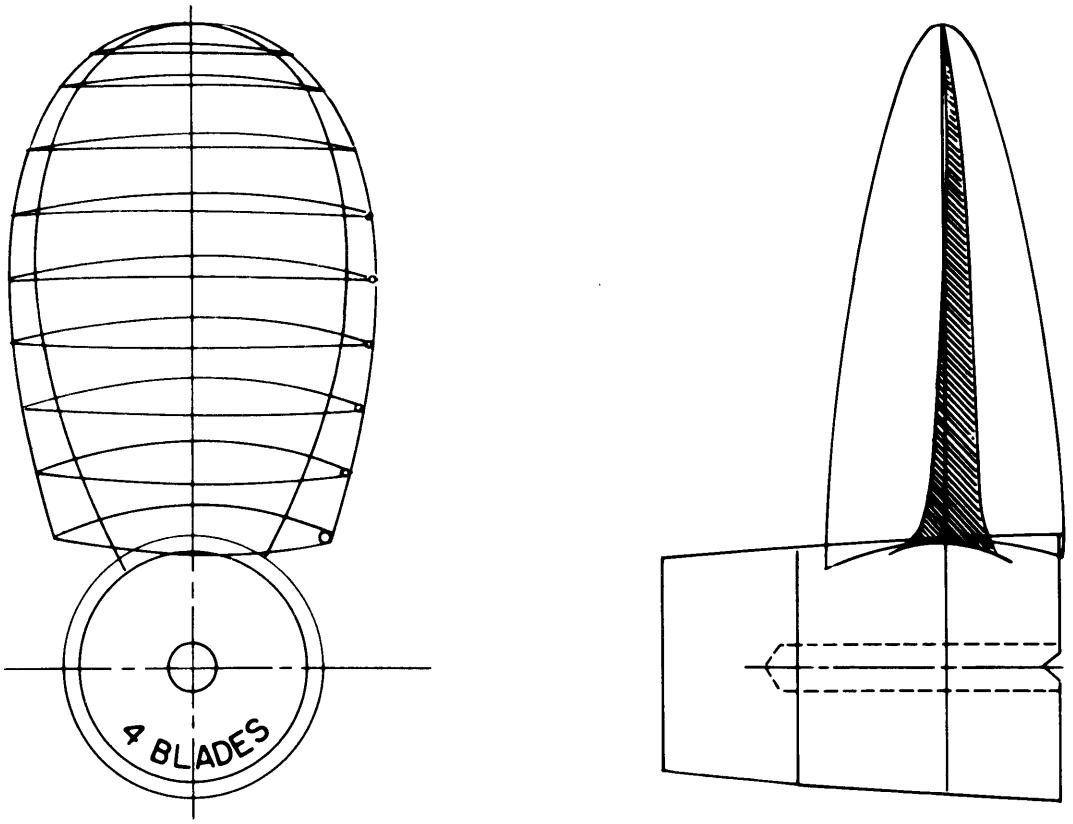

Figure 1 (b) - Drawing of the Wake-Adapted Propeller

NUMBER OF BLADES: Z = 4.0 DIAMETER: D = 21.0'

EXPANDED AREA RATIO: EAR = 0.506 ROTATION: RH

MEAN LINE TYPE: A = 0.800 BLADE OUTLINE: SKEWED

PITCH DISTRIBUTION: LERBS OPTIMUM

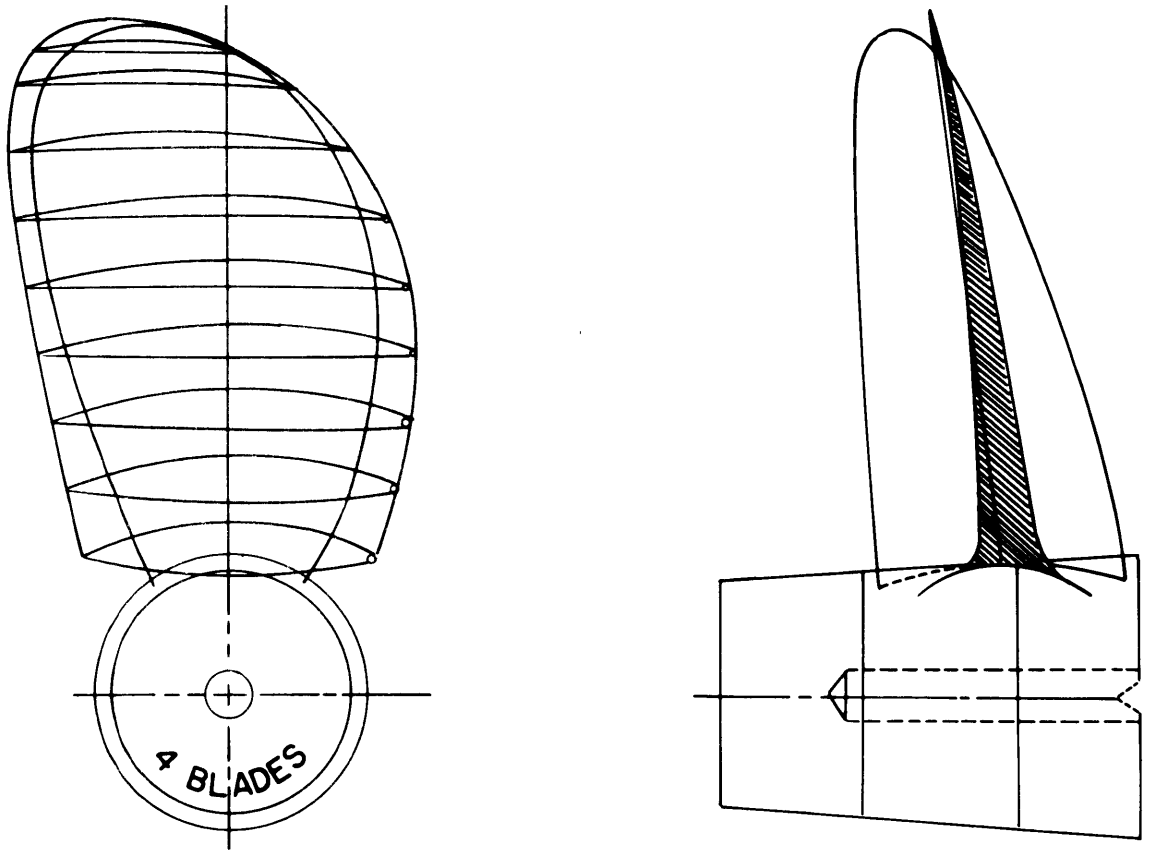

Figure 1 (c) - Drawing of the Wake-Adapted Skewed Propeller

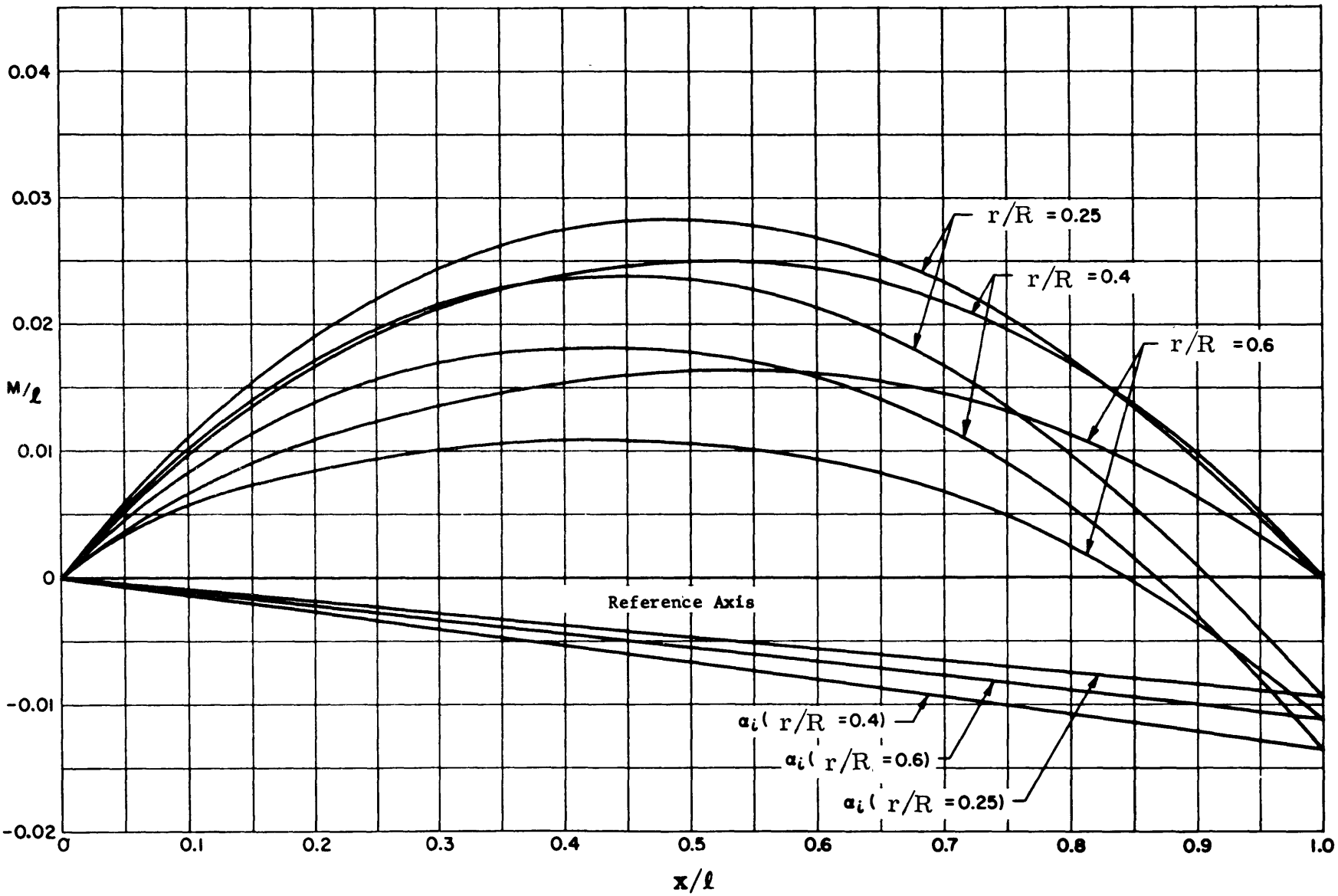

Figure 2 - Correction of the Computed Profile Chord Line up to the Reference Axis

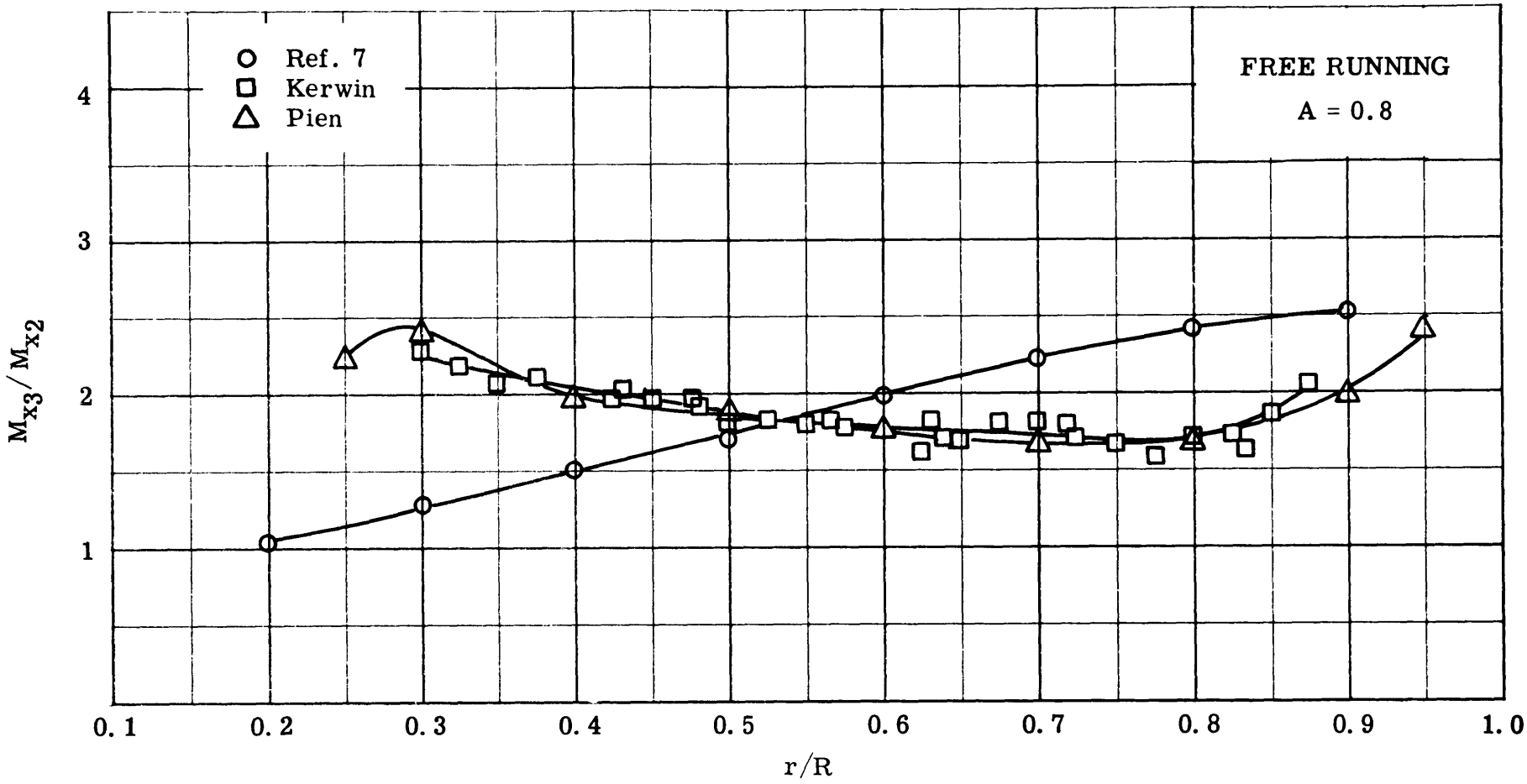

Figure 3 (a) - Comparison of Camber Corrections $\left(\frac{M_{x_3}}{M_{x_2}}\right)$ at Various Nondimensional Radii $\left(\frac{r}{R}\right)$ for Arbitrary Chordwise Load Distribution.

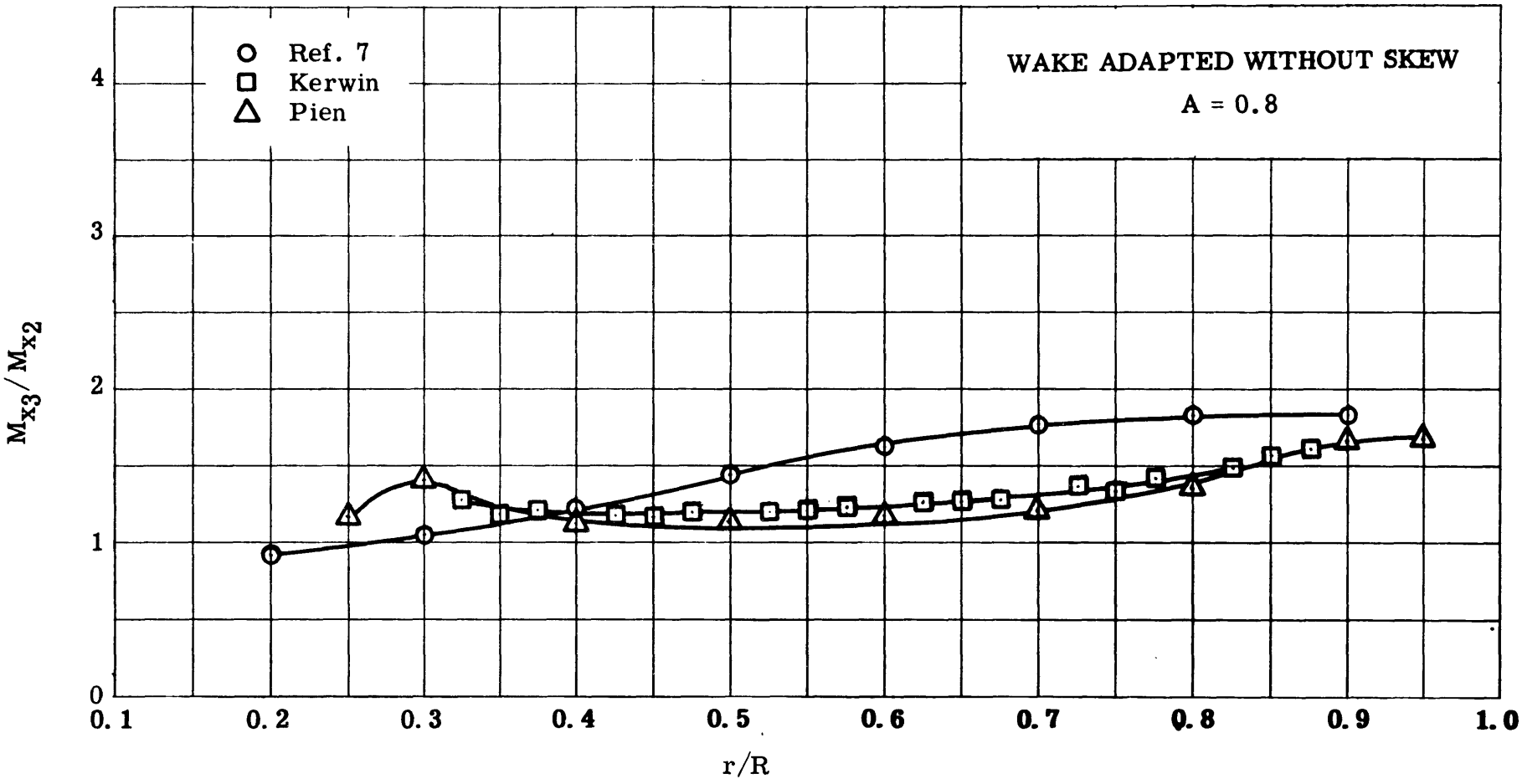

Figure 3 (b) - Comparison of Camber Corrections $\left(\frac{M_{x_3}}{M_{x_2}}\right)$ at Various Nondimensional Radii $\left(\frac{r}{R}\right)$ for Arbitrary Chordwise Load Distribution.

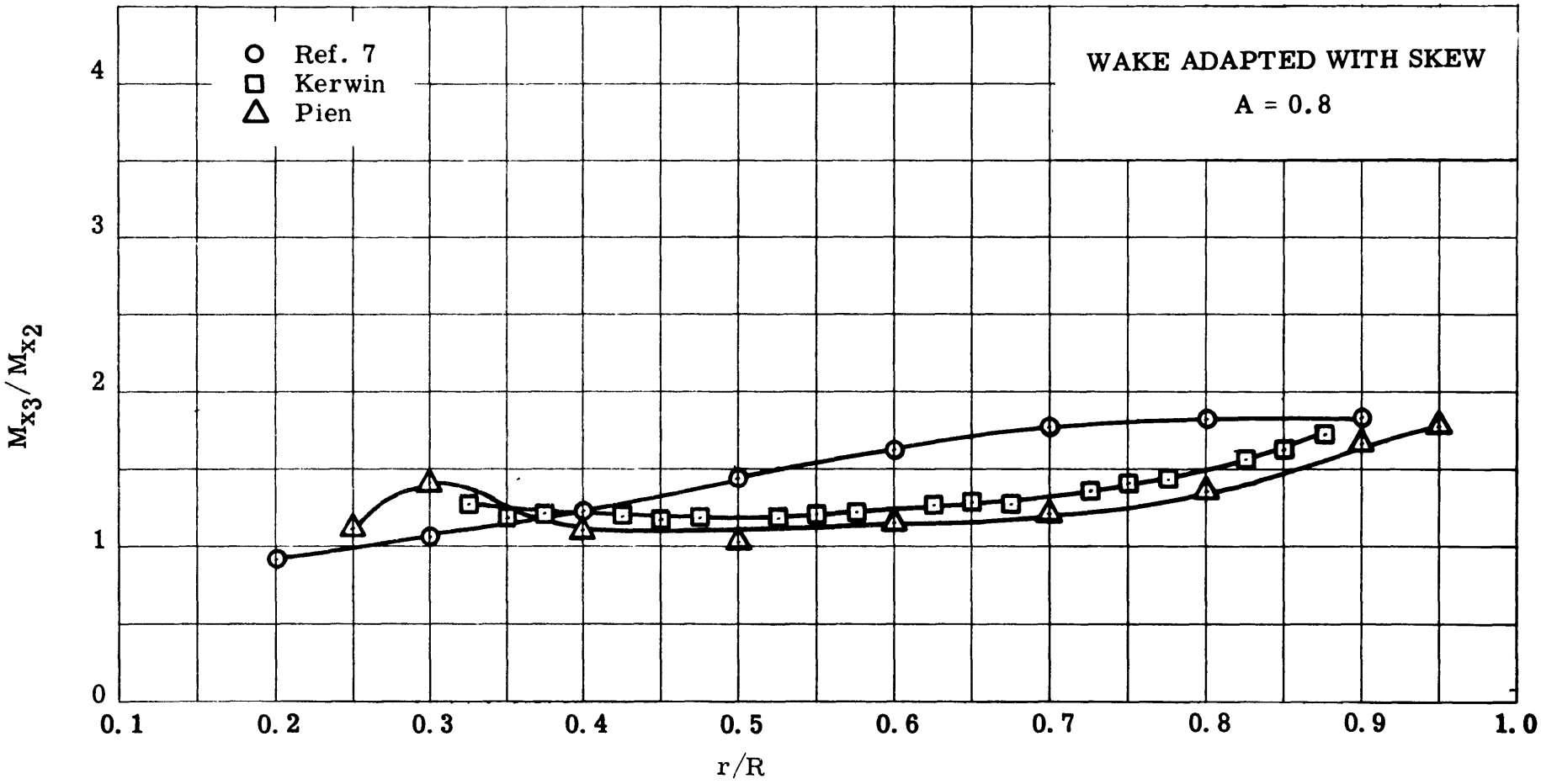

Figure 3 (c) - Comparison of Camber Corrections $\left(\frac{M_{x_3}}{M_{x_2}}\right)$ at Various Nondimensional Radii $\left(\frac{r}{R}\right)$ for Arbitrary Chordwise Load Distribution.

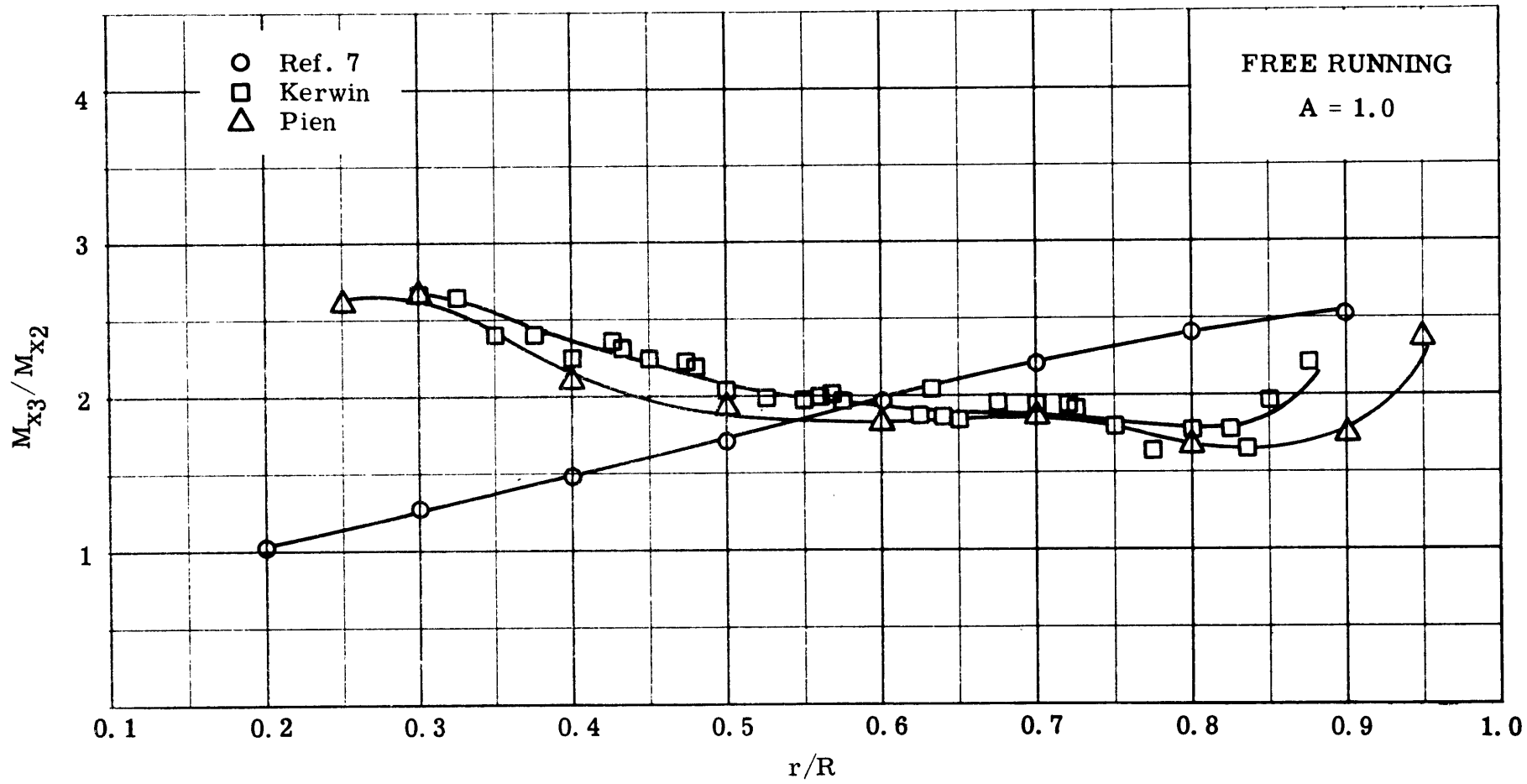

Figure 4 (a) - Comparison of Camber Corrections $\left(\frac{M_{x_3}}{M_{x_2}}\right)$ at Various Nondimensional Radii $\left(\frac{r}{R}\right)$ for Uniform Chordwise Load Distribution.

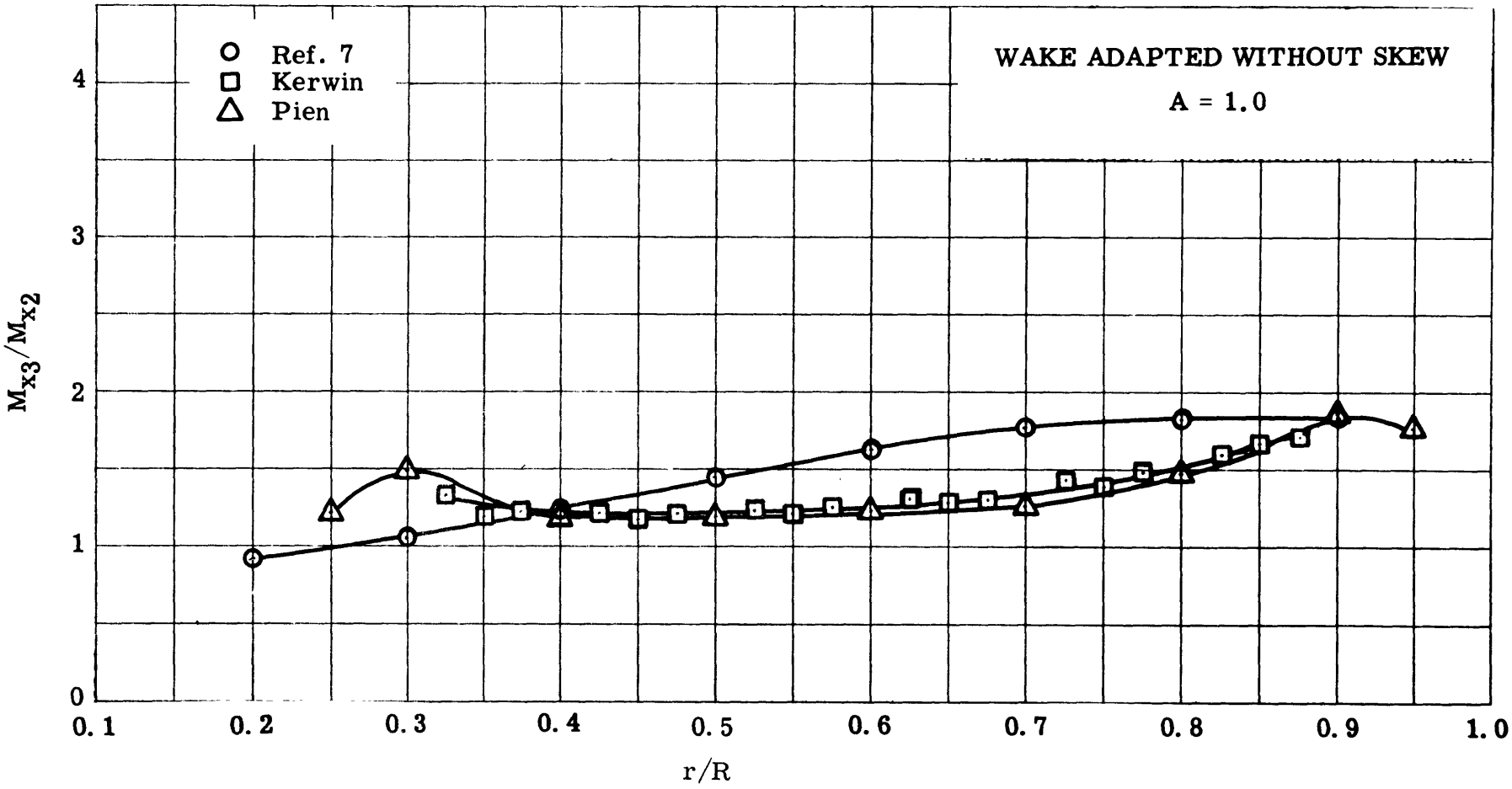

Figure 4 (b) - Comparison of Camber Corrections $\left(\frac{M_{x_3}}{M_{x_2}}\right)$ at Various Nondimensional Radii $\left(\frac{r}{R}\right)$ for Uniform Chordwise Load Distribution.

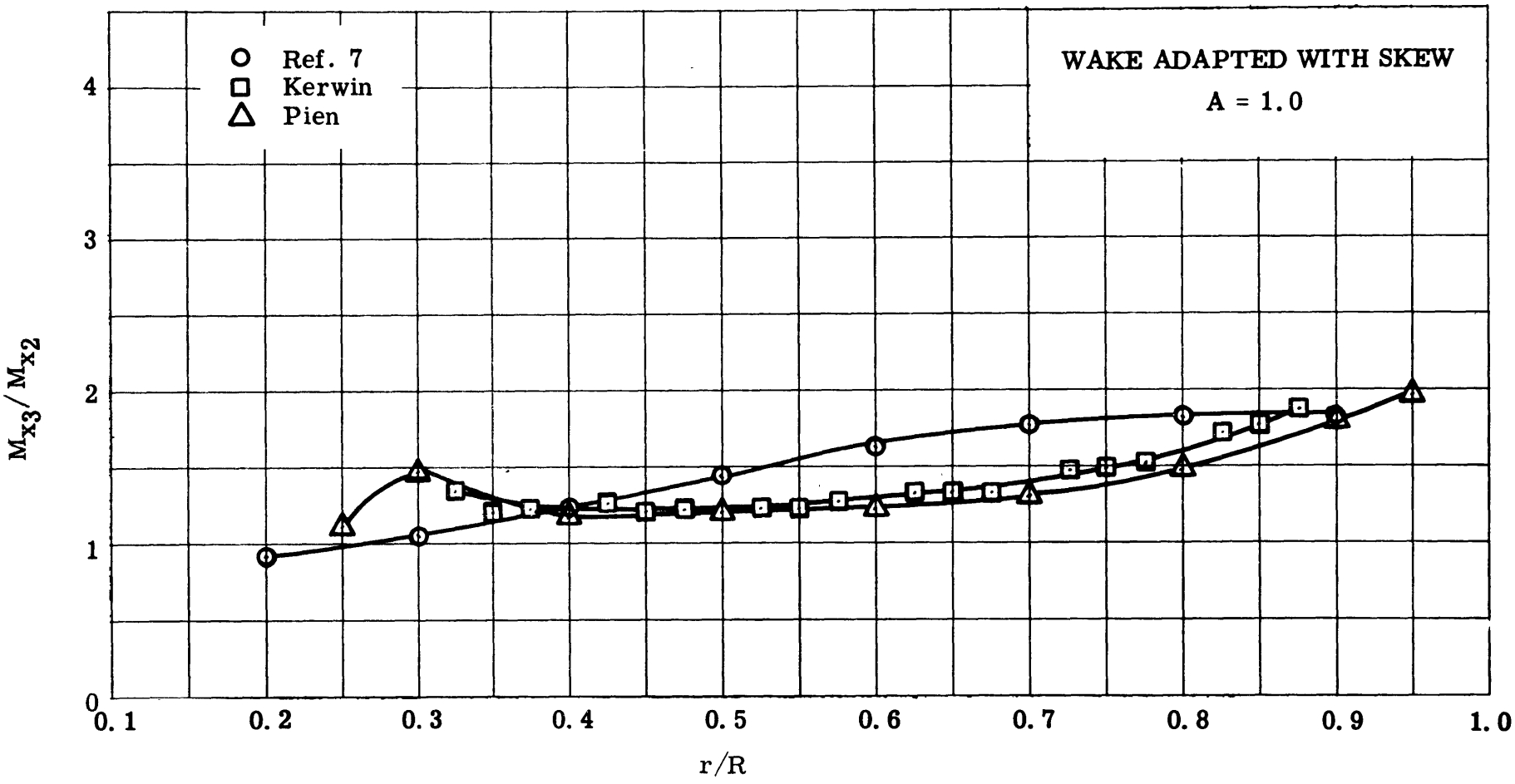

Figure 4 (c) - Comparison of Camber Corrections $\left(\frac{M_{x_3}}{M_{x_2}}\right)$ at Various Nondimensional Radii $\left(\frac{r}{R}\right)$ for Uniform Chordwise Load Distribution.

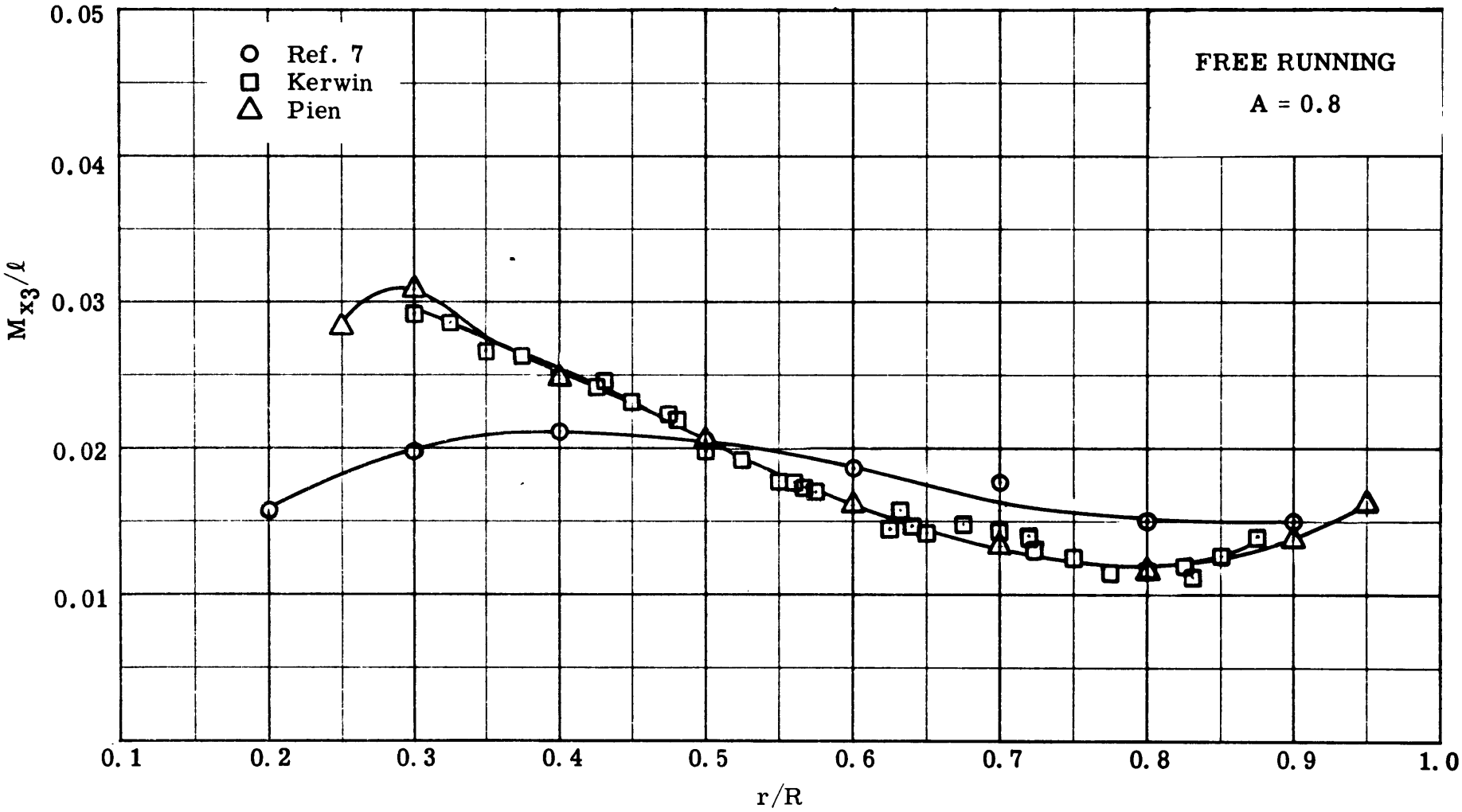

Figure 5 (a) - Comparison of Maximum Camber Ratios $\left(\frac{M_{x3}}{\ell}\right)$ at Various Nondimensional Radii $\left(\frac{r}{R}\right)$ for Arbitrary Chordwise Load Distribution.

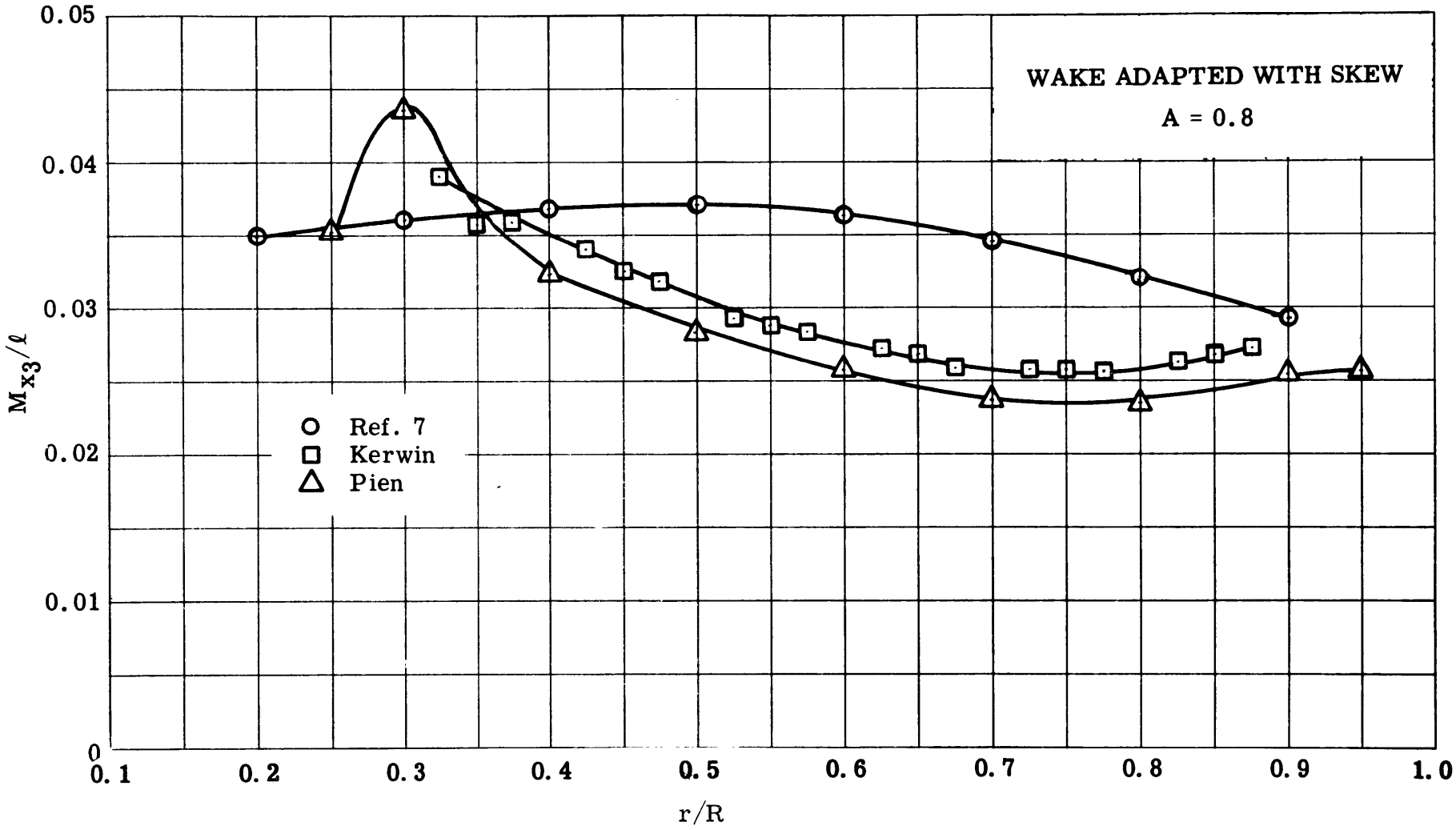

Figure 5 (c) - Comparison of Maximum Camber Ratios $\left(\frac{M_{x3}}{\ell}\right)$ at Various Nondimensional Radii $\left(\frac{r}{R}\right)$ for Arbitrary Chordwise Load Distribution.

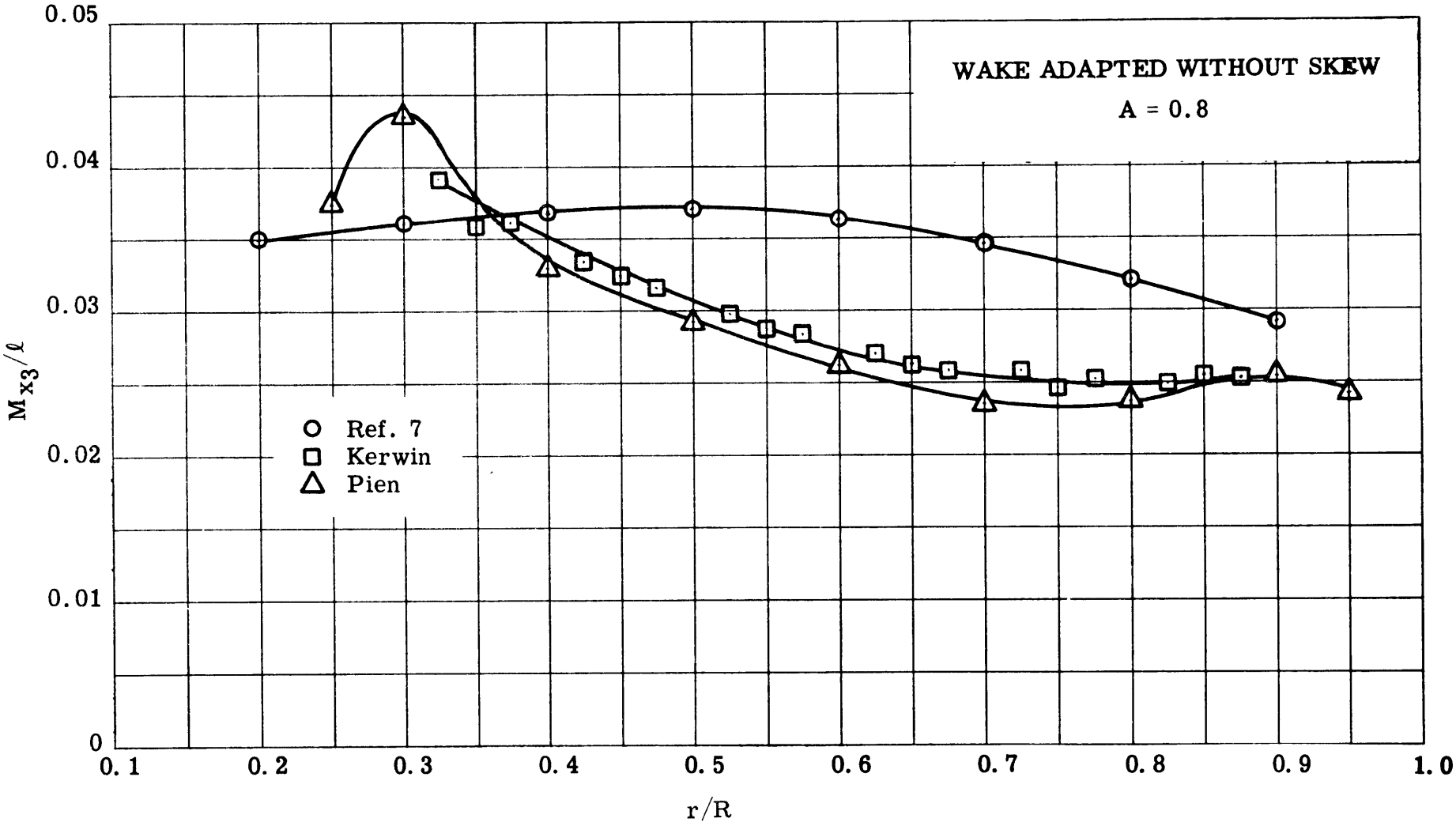

Figure 5 (b) - Comparison of Maximum Camber Ratios $\left(\frac{M_{x3}}{\ell}\right)$ at Various Nondimensional Radii $\left(\frac{r}{R}\right)$ for Arbitrary Chordwise Load Distribution.

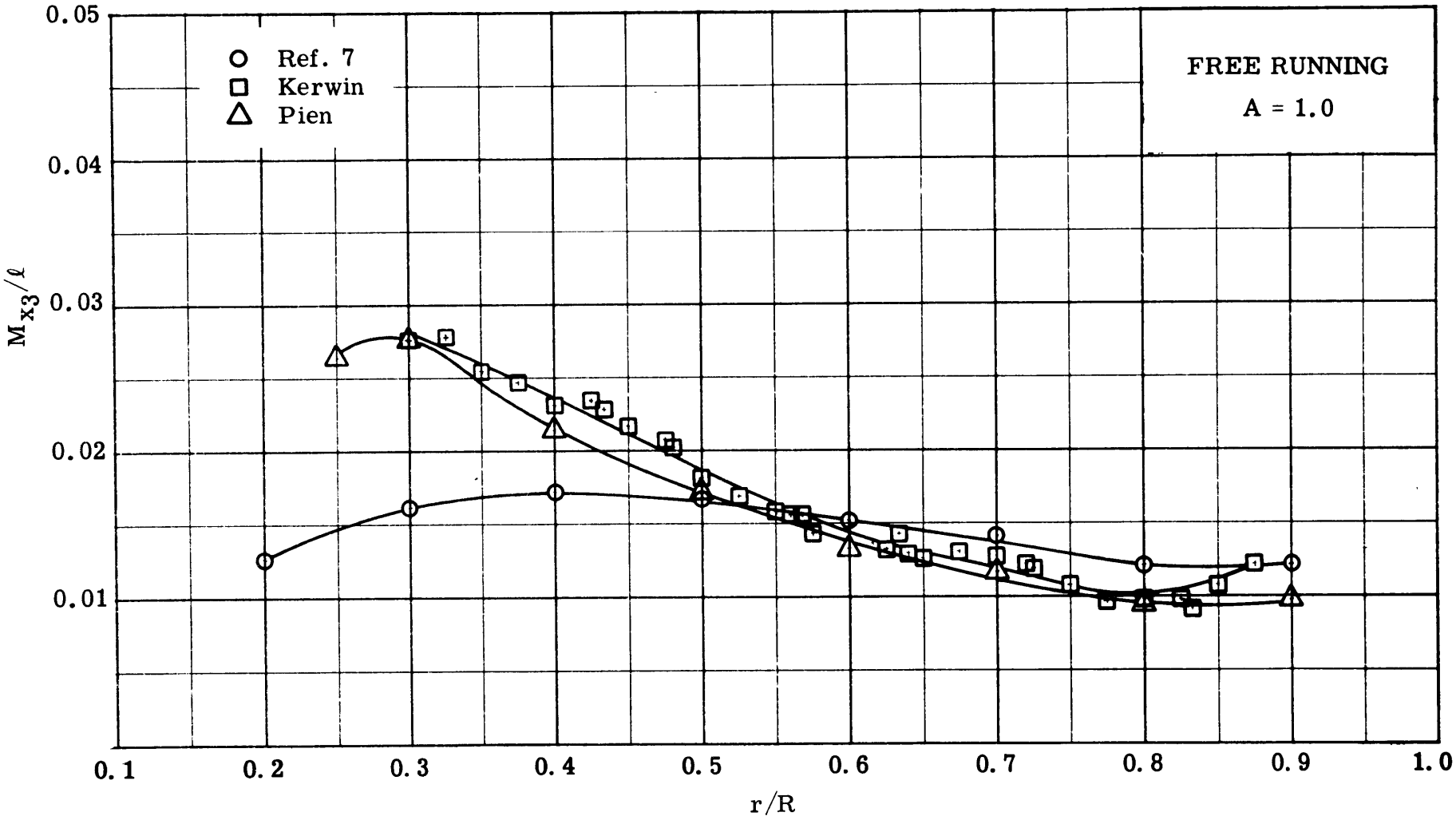

Figure 6 (a) - Comparison of Maximum Camber Ratios $\left(\frac{M_{x3}}{\ell}\right)$ at Various Nondimensional Radii $\left(\frac{r}{R}\right)$ for Uniform Chordwise Load Distribution.

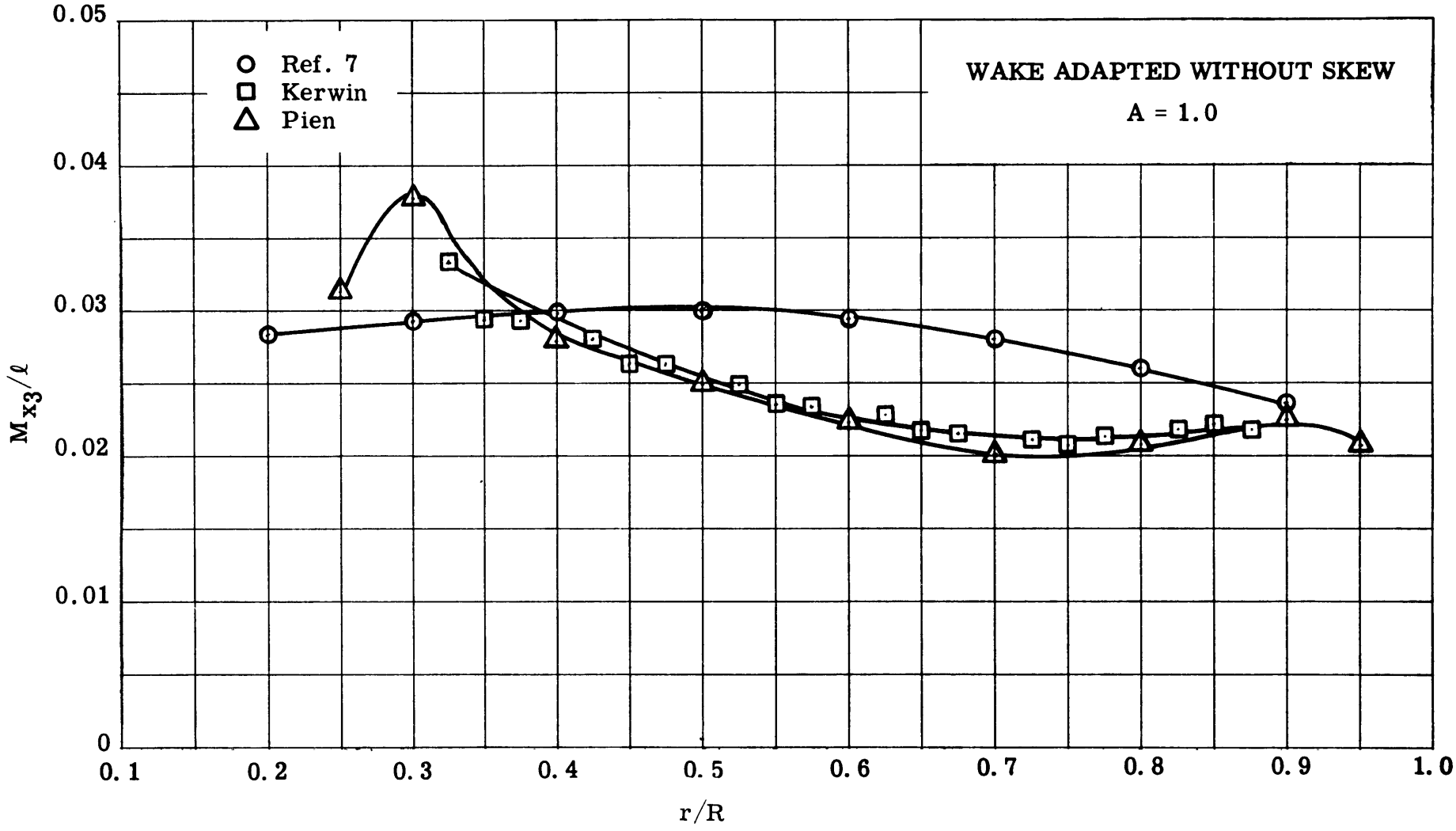

Figure 6 (b) - Comparison of Maximum Camber Ratios $\left(\frac{M_{x3}}{\ell}\right)$ at Various Nondimensional Radii $\left(\frac{r}{R}\right)$ for Uniform Chordwise Load Distribution.

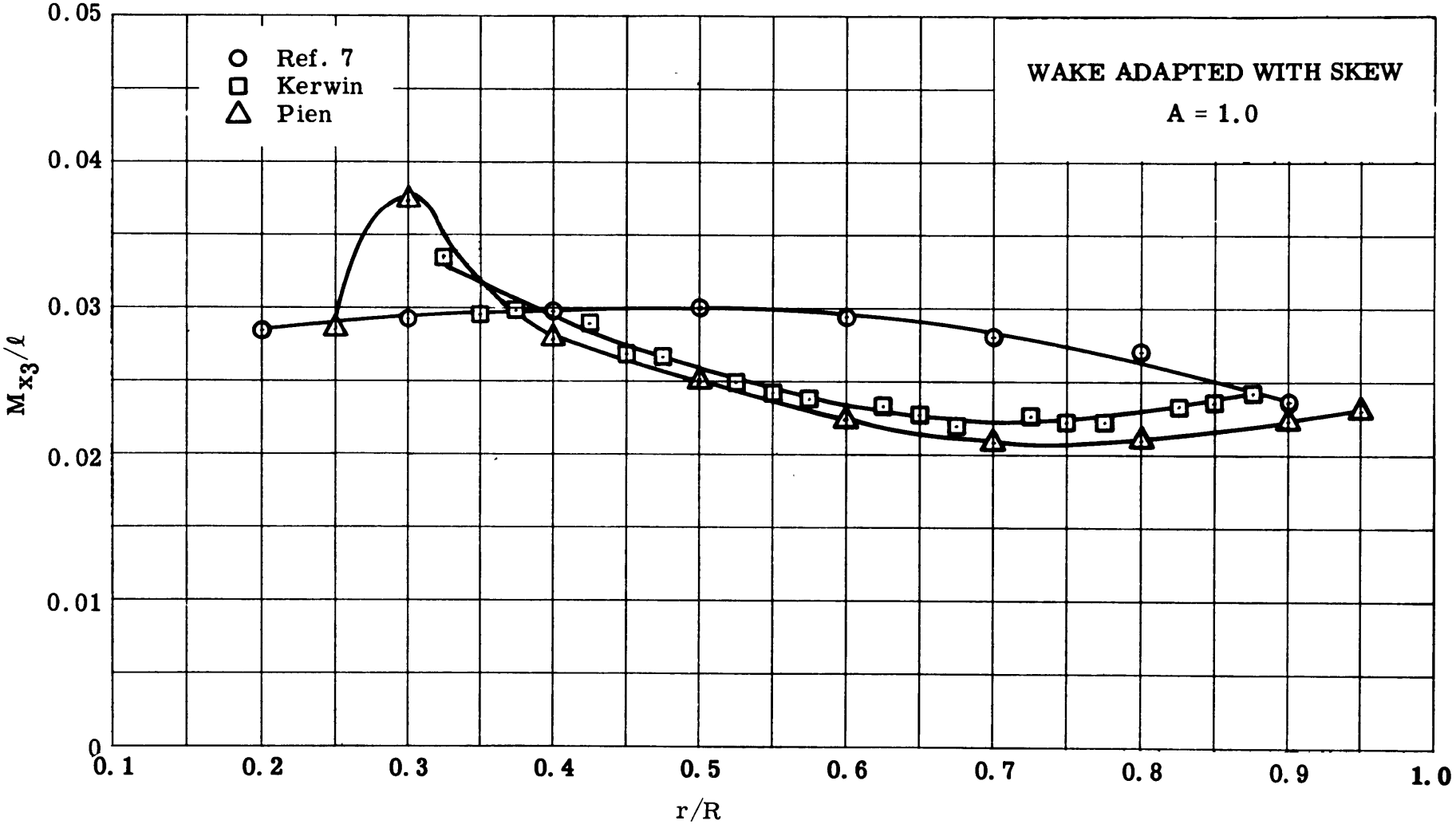

Figure 6 (c) - Comparison of Maximum Camber Ratios $\left(\frac{M_x}{\ell}\right)$ at Various Nondimensional Radii $\left(\frac{r}{R}\right)$ for Uniform Chordwise Load Distribution

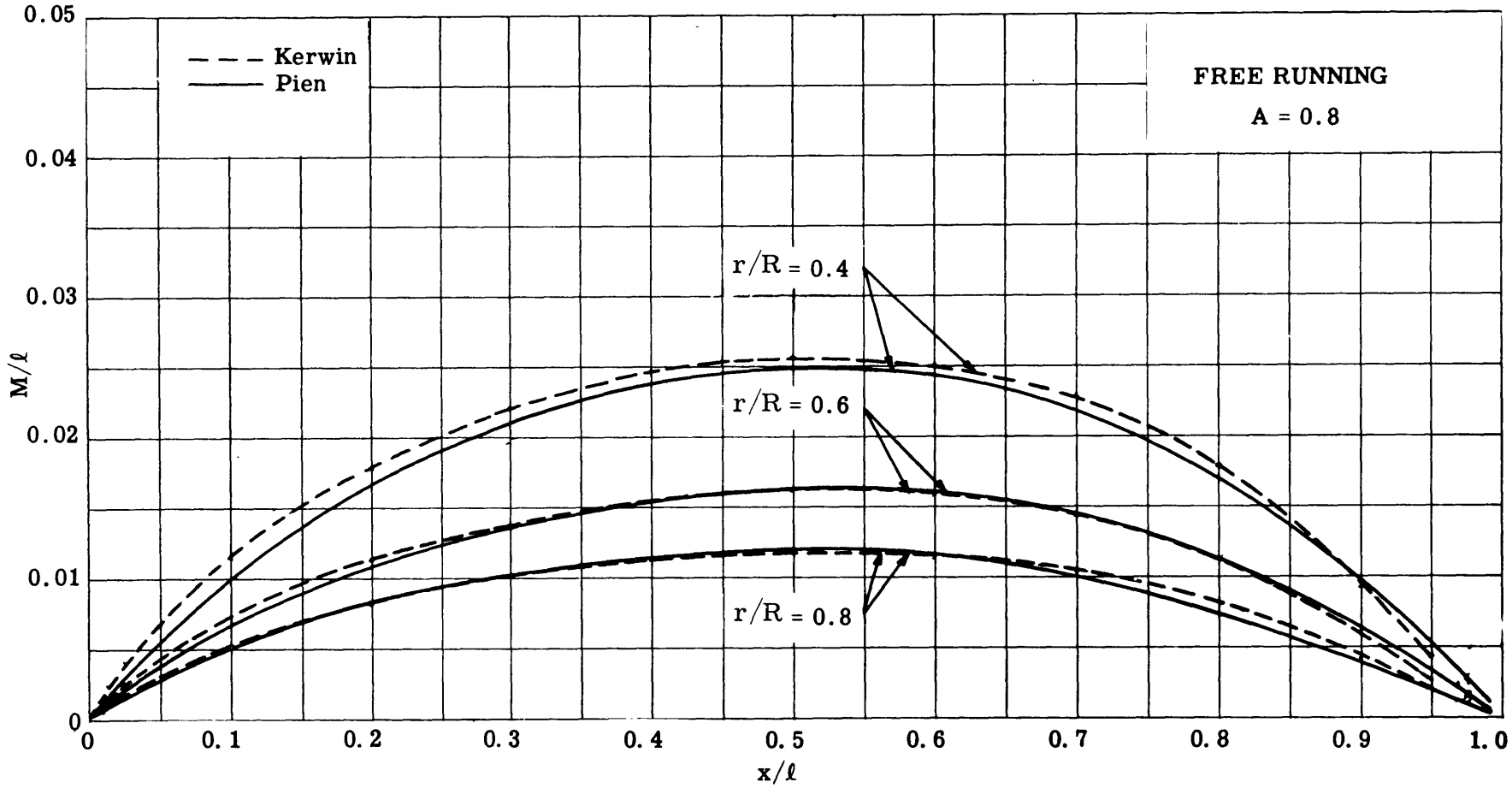

Figure 7 (a) - Chordwise Comparison of Camber Ratios $\left(\frac{M}{\ell}\right)$ at Fraction of Chord $\left(\frac{x}{\ell}\right)$ for Arbitrary Chordwise Load Distribution.

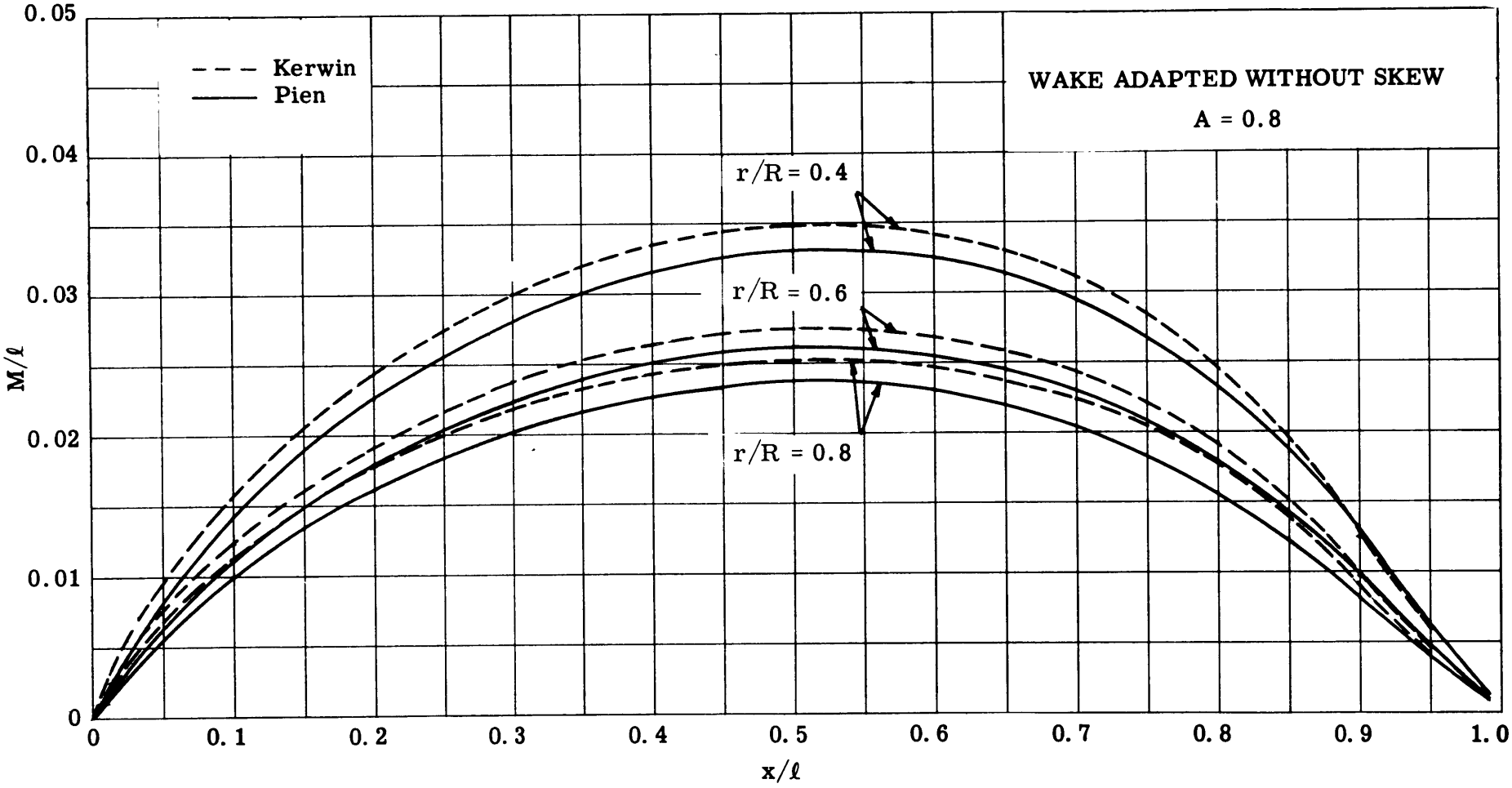

Figure 7 (b) - Chordwise Comparison of Camber Ratios $\left(\frac{M}{\ell}\right)$ at Fraction of Chord $\left(\frac{x}{\ell}\right)$

for Arbitrary Chordwise Load Distribution.

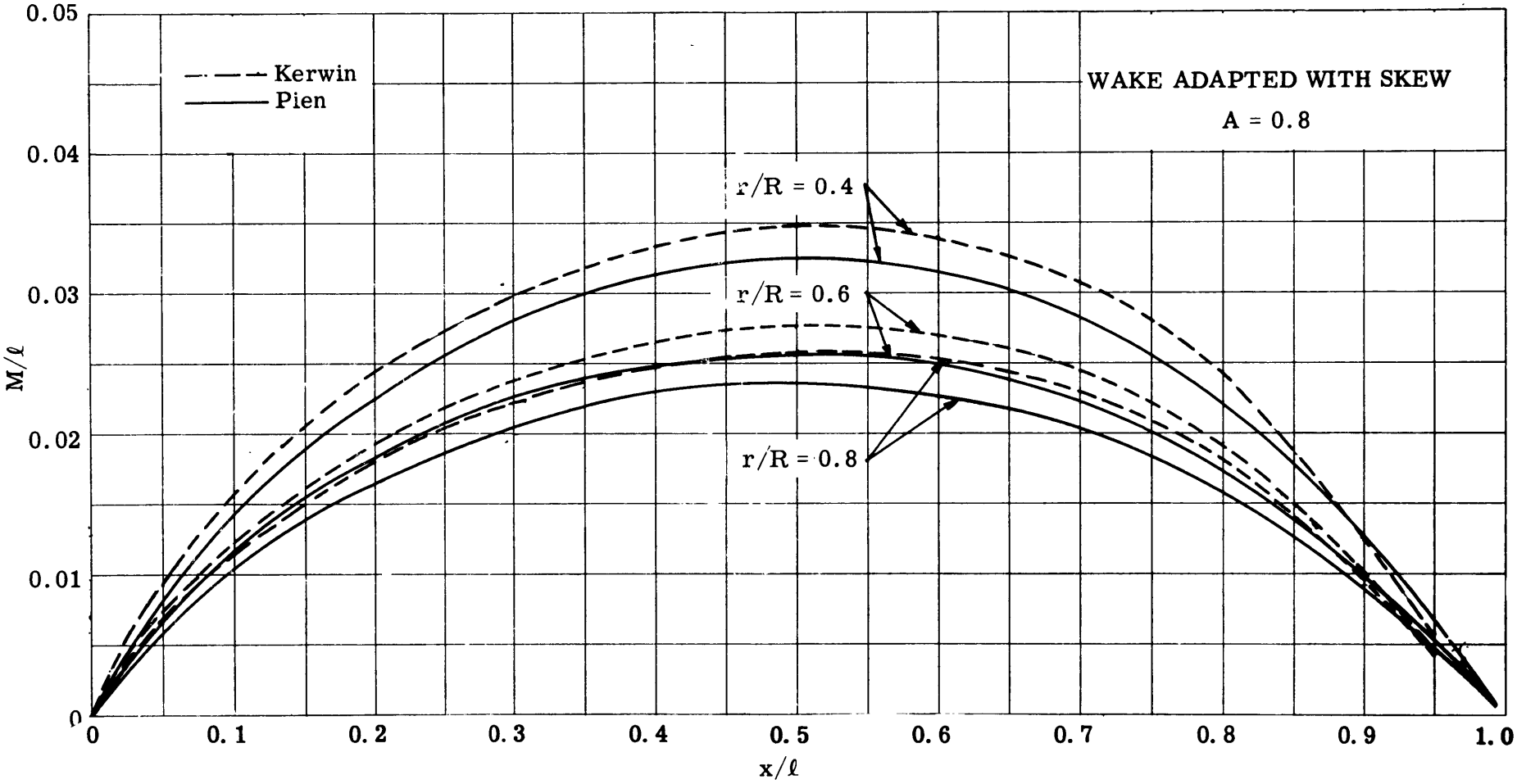

Figure 7 (c) - Chordwise Comparison of Camber Ratios $\left(\frac{M}{\ell}\right)$ at Fraction of Chord $\left(\frac{x}{\ell}\right)$ for Arbitrary Chordwise Load Distribution.

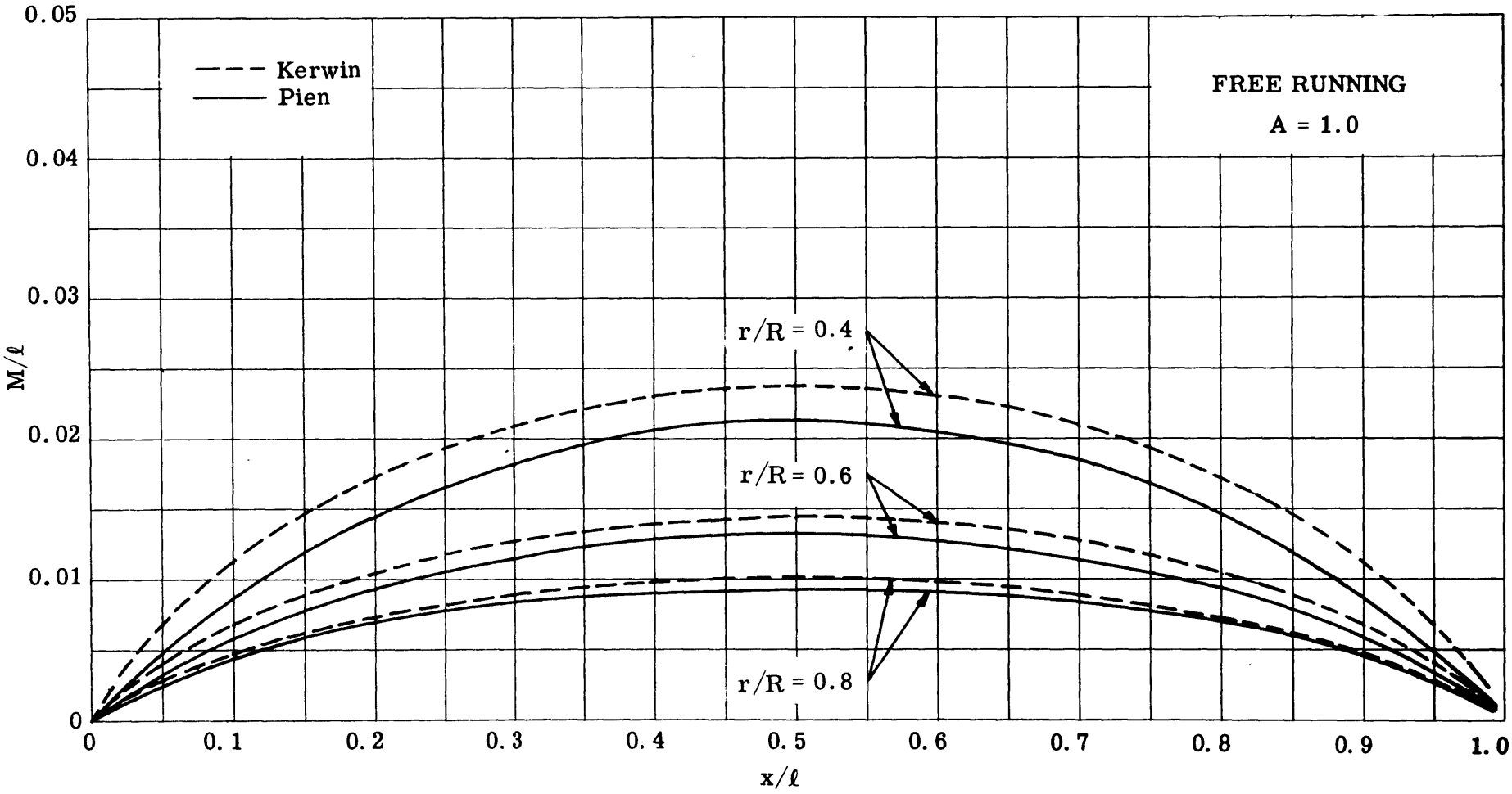

Figure 8 (a) - Chordwise Comparison of Camber Ratios $\left(\frac{M}{\ell}\right)$ at Fraction of Chord $\left(\frac{x}{\ell}\right)$ for Uniform Chordwise Load Distribution.

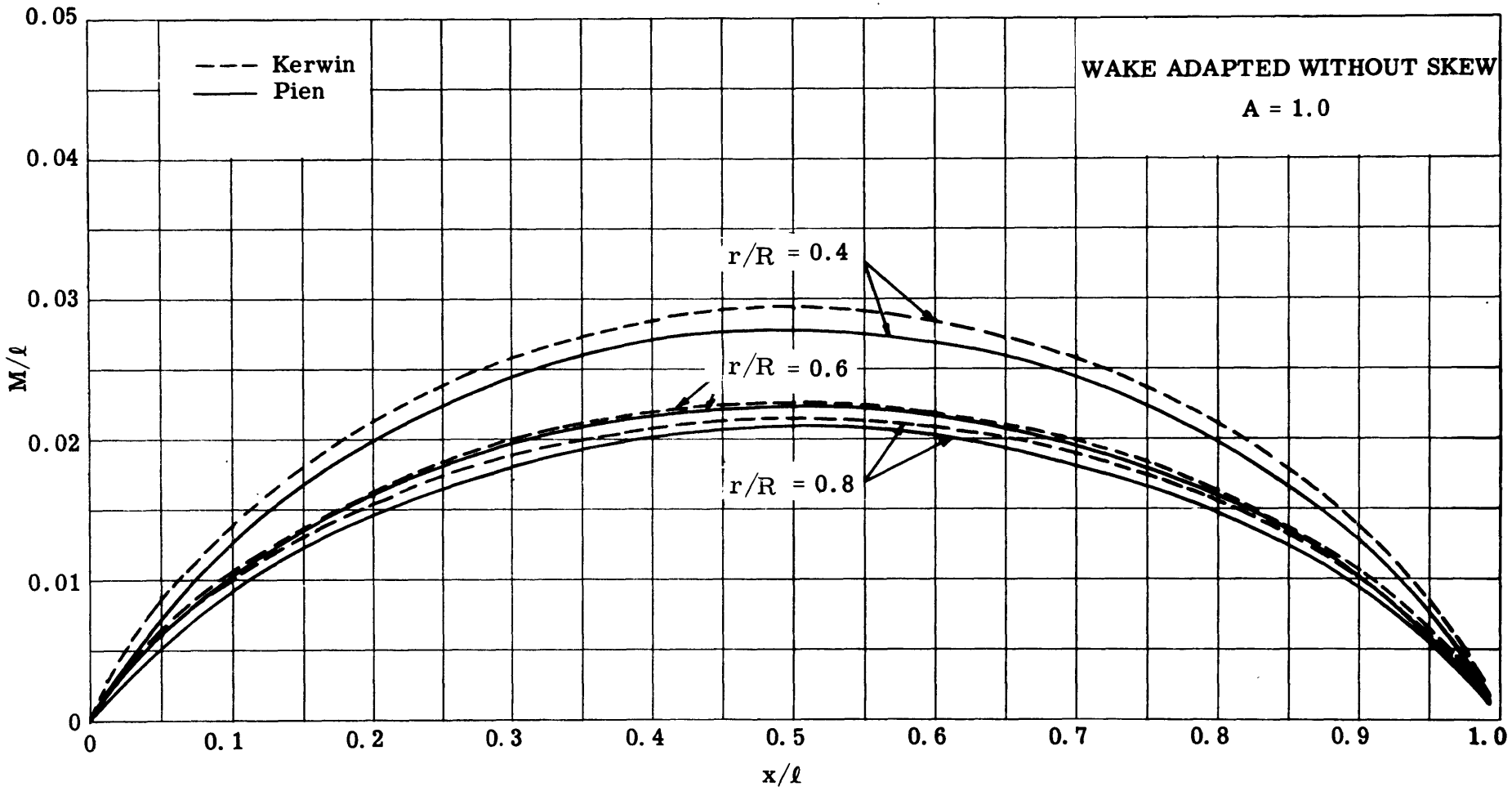

Figure 8 (b) - Chordwise Comparison of Camber Ratios $\left(\frac{M}{\ell}\right)$ at Fraction of Chord $\left(\frac{x}{\ell}\right)$

for Uniform Chordwise Load Distribution.

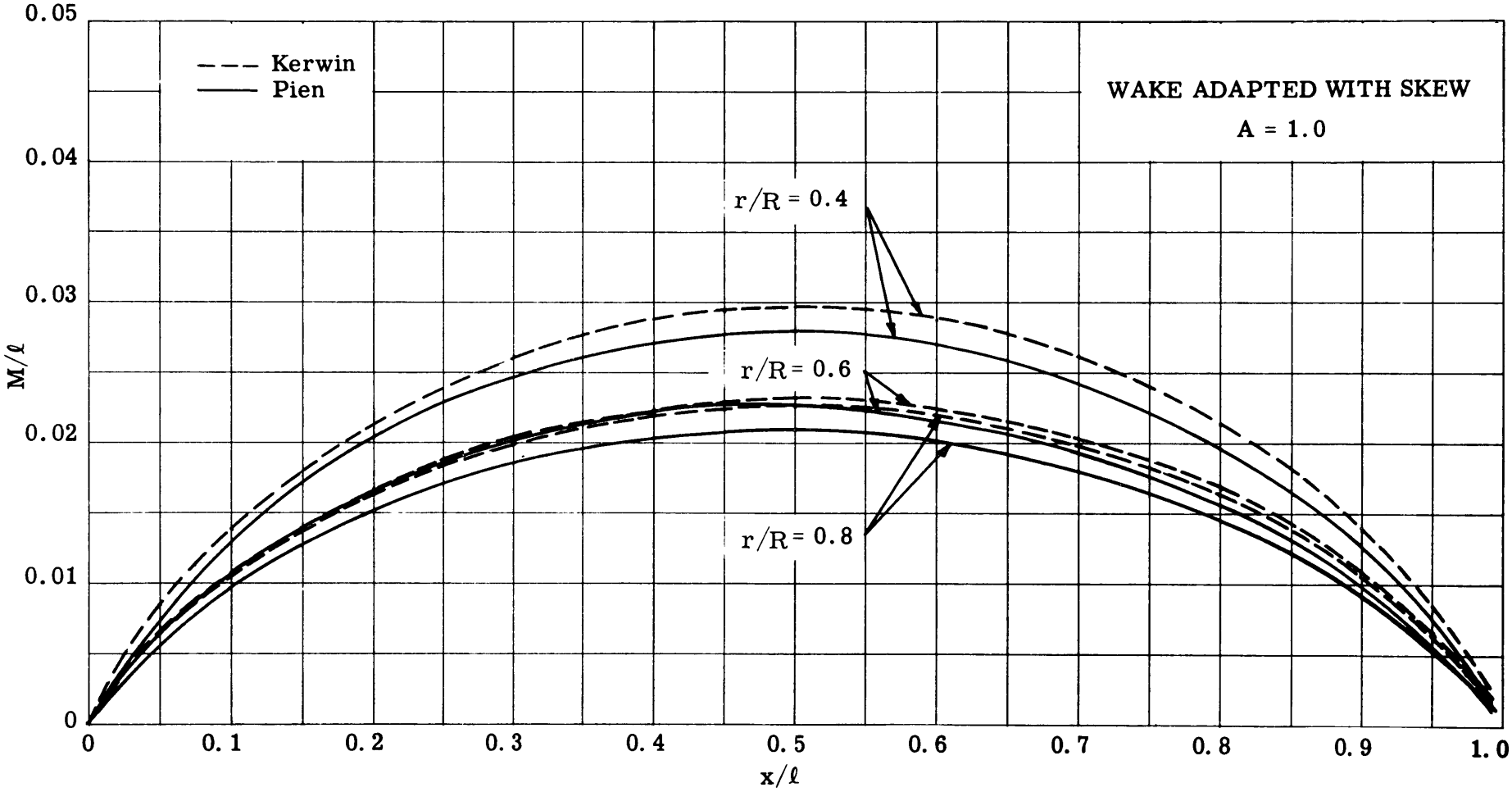

Figure 8 (c) - Chordwise Comparison of Camber Ratios $\left(\frac{M}{\ell}\right)$ at Fraction of Chord $\left(\frac{x}{\ell}\right)$

for Uniform Chordwise Load Distribution.

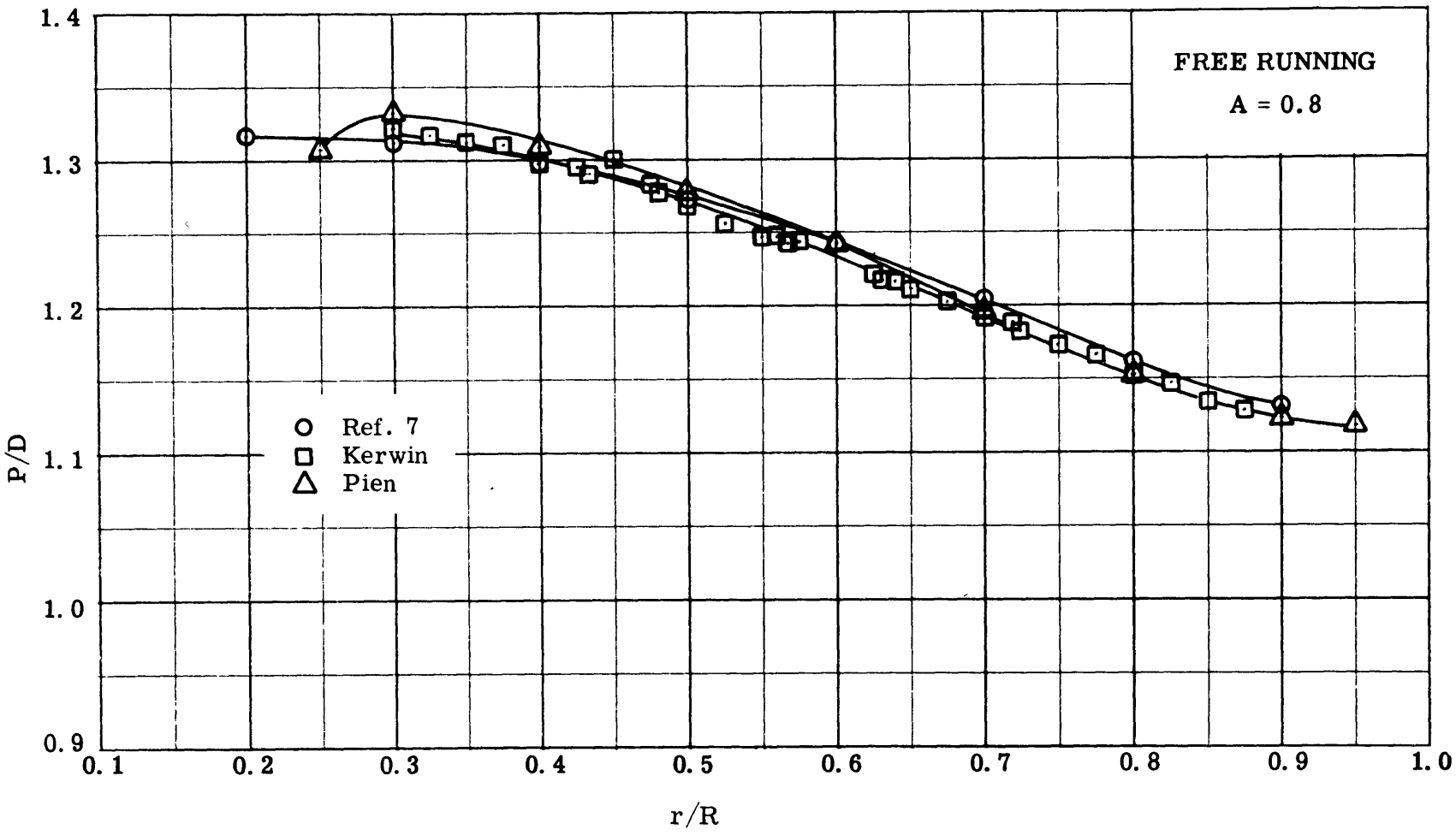

Figure 9 (a) - Comparison of Pitch Ratios $\left(\frac{P}{D}\right)$ at Various Nondimensional Radii $\left(\frac{r}{R}\right)$ for Arbitrary Chordwise Load Distribution.

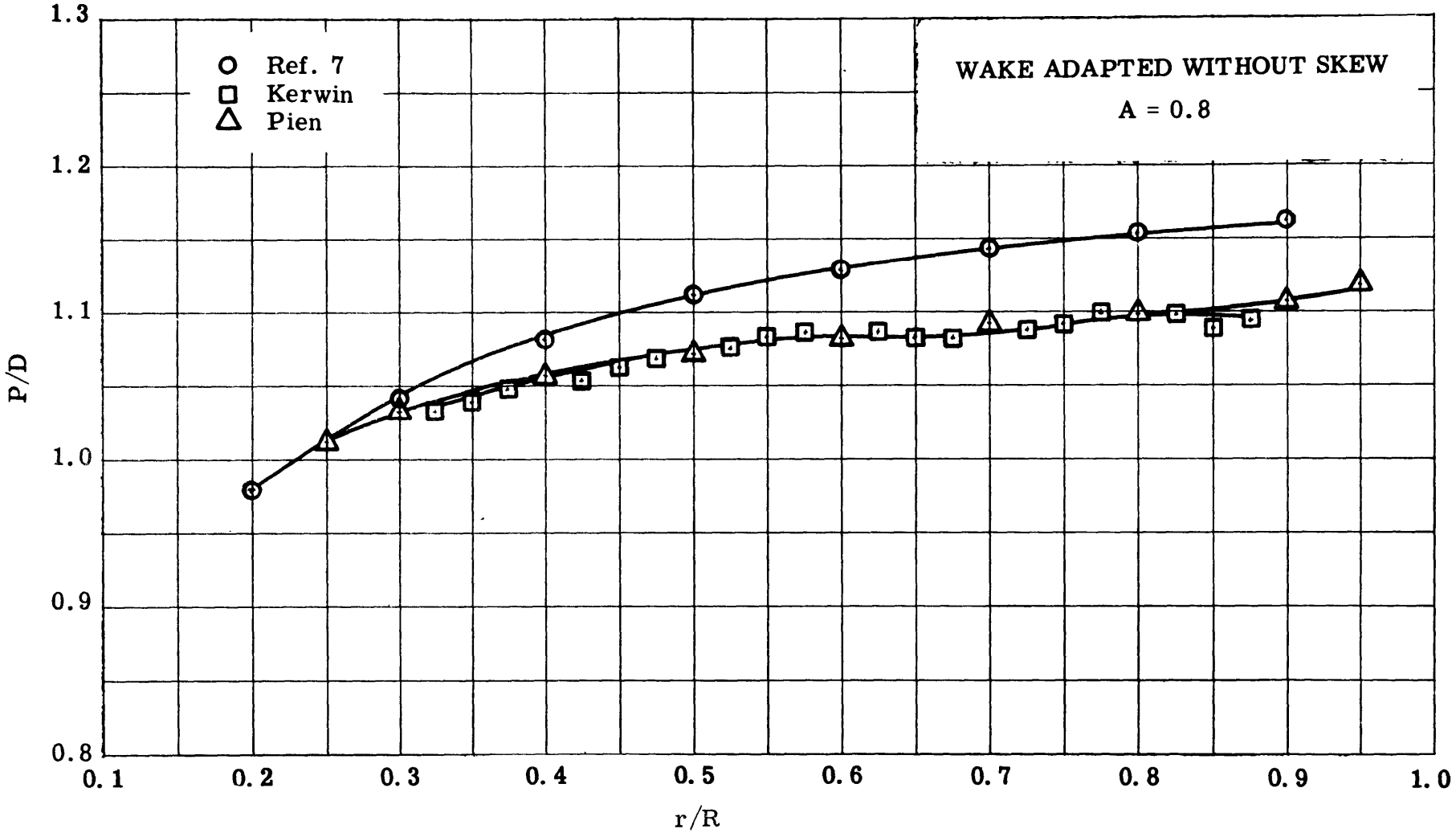

Figure 9 (b) - Comparison of Pitch Ratios $\left(\frac{P}{D}\right)$ at Various Nondimensional Radii $\left(\frac{r}{R}\right)$ for Arbitrary Chordwise Load Distribution.

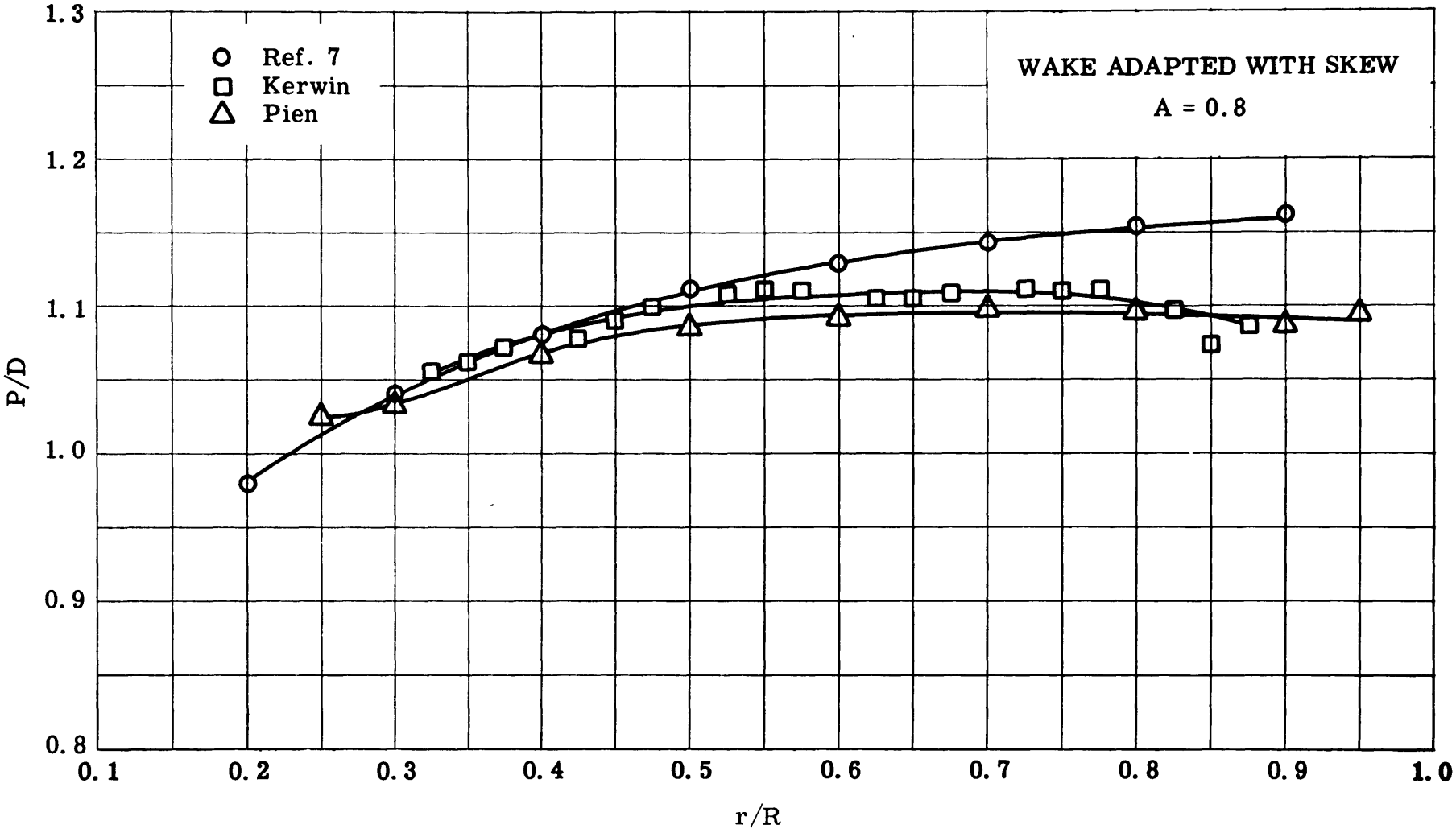

Figure 9 (c) - Comparison of Pitch Ratios $\left(\frac{P}{D}\right)$ at Various Nondimensional Radii $\left(\frac{r}{R}\right)$ for Arbitrary Chordwise Load Distribution.

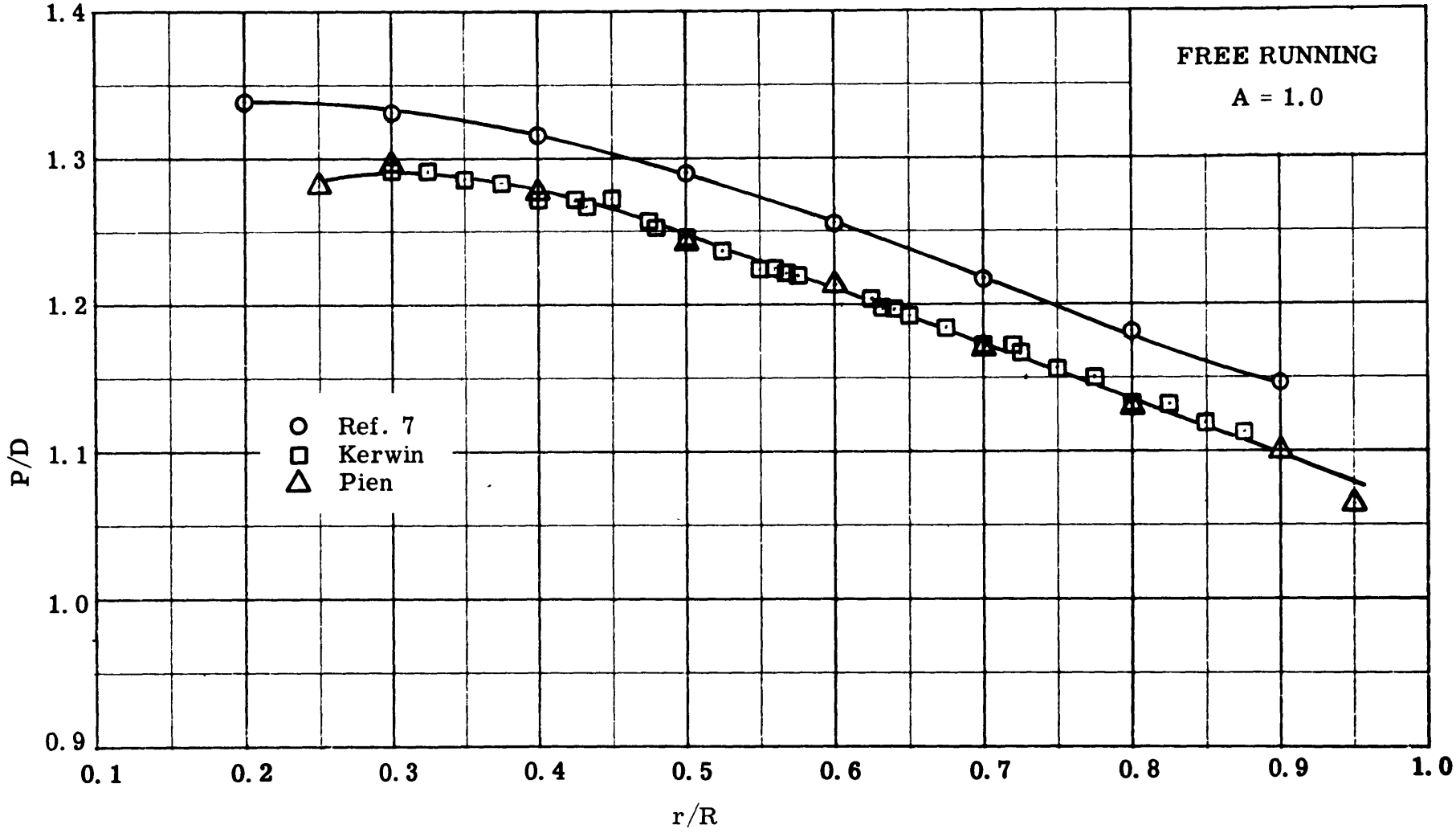

Figure 10 (a) - Comparison of Pitch Ratios $\left(\frac{P}{D}\right)$ at Various Nondimensional Radii $\left(\frac{r}{R}\right)$ for Uniform Chordwise Load Distribution.

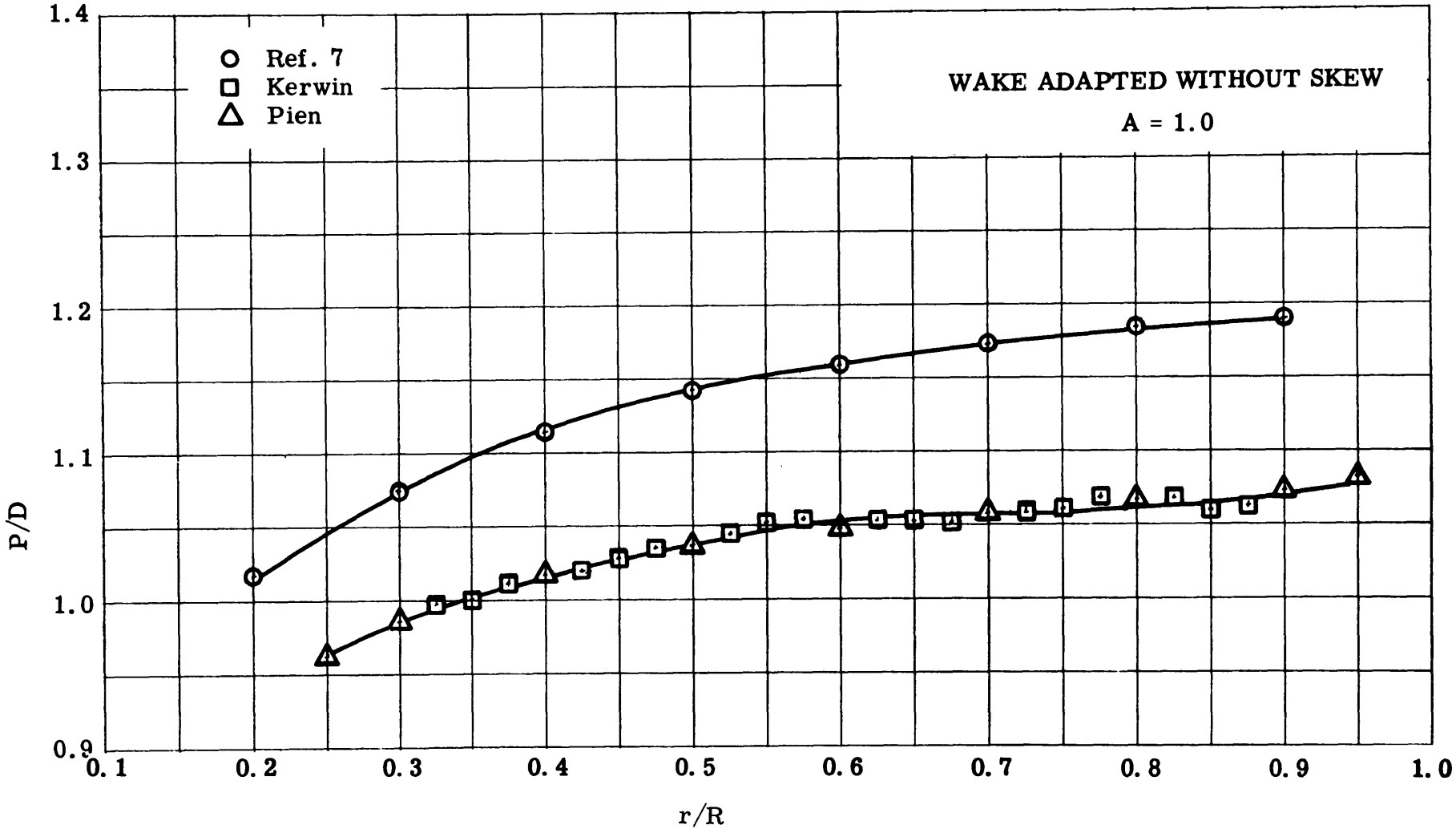

Figure 10 (b) - Comparison of Pitch Ratios $\left(\frac{P}{D}\right)$ at Various Nondimensional Radii $\left(\frac{r}{R}\right)$ for Uniform Chordwise Load Distribution.

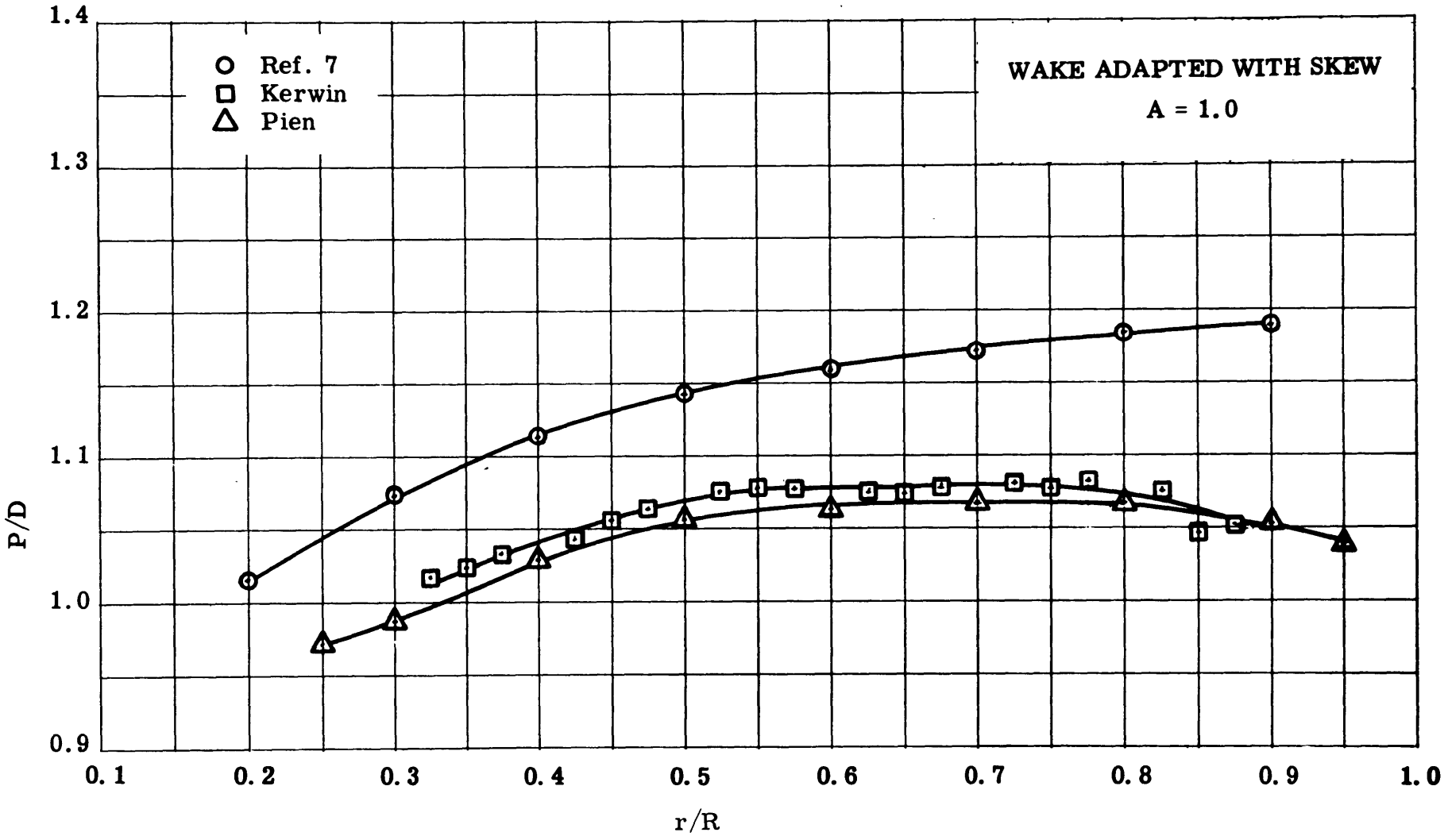

Figure 10 (c) - Comparison of Pitch Ratios $\left(\frac{P}{D}\right)$ at Various Nondimensional Radii $\left(\frac{r}{R}\right)$ for Uniform Chordwise Load Distribution.

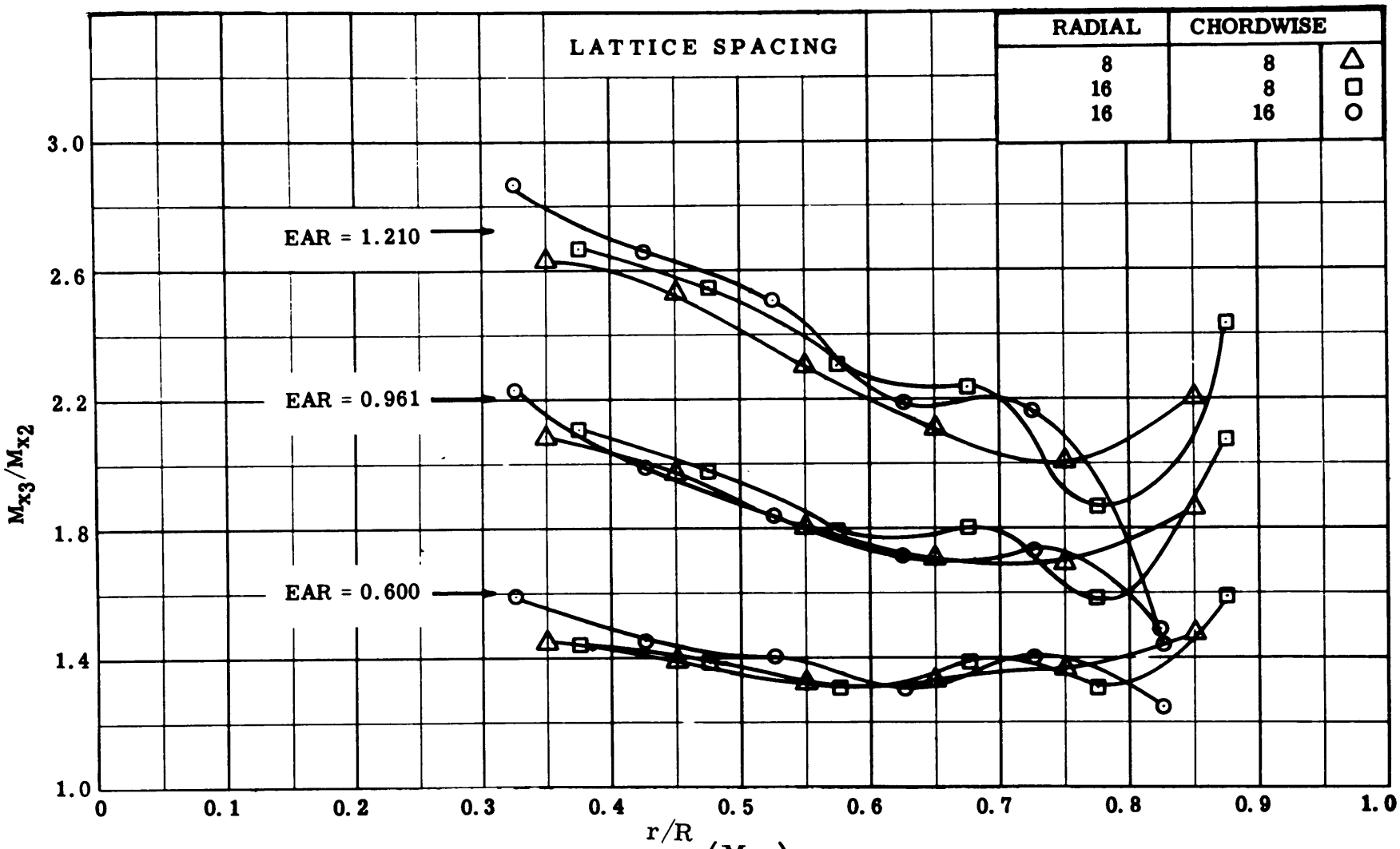

Figure 11 - Comparison of Camber Corrections $\left(\frac{M_{x3}}{M_{x2}}\right)$ Obtained with Several Different Lattice Spacings for Propellers with Different Expanded Area Ratios (EAR).

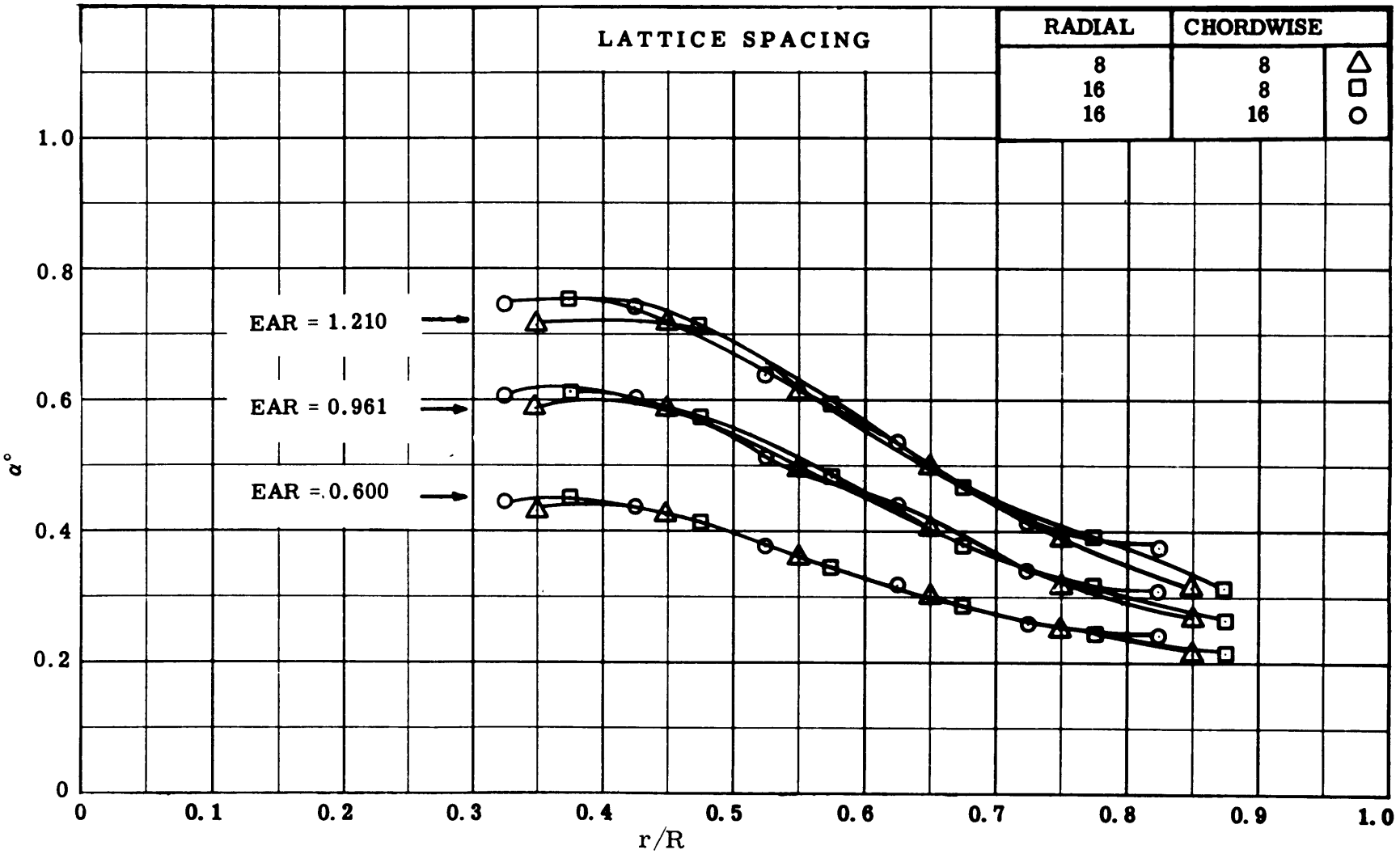

Figure 12 - Comparison of Incidence Corrections $\left(\alpha_i^{(1)}\right)$ Obtained with Several Different Lattice Spacings for Propellers with Different Expanded Area Ratios (EAR).

INITIAL DISTRIBUTION

Copies	
11	CHBUSHIPS
	1 Lab Mgt (Code 320)
	3 Tech Info Br (Code 210-L)
	1 Appl Res (Code 340)
	1 Prelim Des (Code 420)
	1 Mach Des (Code 430)
	1 Mach Sci & Res (Code 436)
	1 Hull Des (Code 440)
	2 Prop Shaft & Brng (Code 644)
3	CHBUWEPS
	1 Library (DLI 3)
	1 Res & Components (RuSD-342)
	1 Hydro Propul Sec (RuTO-32)
3	CHONR
	2 Fluid Dyn (Code 438)
	1 Undersea Programs (Code 466)
1	CDR, USNOTS, Pasadena Annex
1	CDR, USNOL
1	DIR, USNRL
1	DIR, USNMEL
1	SUPT, USNAVPGSCOL
1	ADMIN, Maritime Adm
1	Gibbs and Cox, Inc
1	HD, Dept NAME, MIT
1	Hydro Lab, CIT
1	DIR, Iowa Inst of Hydraulic Res
1	DIR, St. Anthony Falls Hydraulic Lab
1	PIB, Dept of Aero Eng & Appl Mech
1	DIR, ORL
1	Aerojet General Corp., Azusa, Calif
1	DIR, Davidson Lab, SIT
1	DIR, Inst of Eng Res, Univ of Calif
1	HD, Dept NAME, Univ of Mich
1	ADMIN, INST NAVARCH, Webb
2	University of Calif, Berkeley
	1 Library
	1 Head, Dept NAVARCH
1	Hydronautics
20	DDC
1	SNAME
1	George G. Sharp, Inc
1	Grumman Aircraft
1	Boeing Aircraft Corp
1	Electric Boat Div, General Dyn Corp., Groton
1	Lockheed, Sunnyvale
1	Oceanics
1	NASA, Hdqtrs Manned Space Flights, Attention Dr. W. L. Haberman

Unclassified

Security Classification

DOCUMENT CONTROL DATA - R&D

(Security classification of title, body of abstract and indexing annotation must be entered when the overall report is classified)

1. ORIGINATING ACTIVITY *(Corporate author)*: Bureau of Ships

2a. REPORT SECURITY CLASSIFICATION: Unclassified

2b GROUP:

3. REPORT TITLE: A Comparison of the Lifting-Surface Corrections Calculated by Different Methods for Three Propeller Designs

4. DESCRIPTIVE NOTES *(Type of report and inclusive dates)*: Research and Development Report

5. AUTHOR(S) *(Last name, first name, initial)*: Harley, Ernest E.

6. REPORT DATE: September 1965

7a. TOTAL NO. OF PAGES: 61

7b. NO. OF REFS: 17

8a. CONTRACT OR GRANT NO.:

b. PROJECT NO.: S-R009-01-01

c. Task 0101

d.

9a. ORIGINATOR'S REPORT NUMBER(S): 2049

9b. OTHER REPORT NO(S) *(Any other numbers that may be assigned this report)*: None

10. AVAILABILITY/LIMITATION NOTICES: Qualified Requesters May Obtain Copies of This Report From DDC.

11. SUPPLEMENTARY NOTES:

12. SPONSORING MILITARY ACTIVITY: David Taylor Model Basin

13. ABSTRACT

This report presents the results of a comparison of lifting-surface corrections calculated by several numerical methods for three propellers. Specifically, the camber corrections, radial and chordwise distribution of camber, and the propeller pitch ratios are compared. The results of the comparison, presented in nondimensional form, are shown graphically and through tables.

DD FORM 1 JAN 64 1473

Unclassified

Security Classification

14. KEY WORDS	LINK A		LINK B		LINK C	
	ROLE	WT	ROLE	WT	ROLE	WT
Propeller design						
Lifting-surface theories						

INSTRUCTIONS

1. ORIGINATING ACTIVITY: Enter the name and address of the contractor, subcontractor, grantee, Department of Defense activity or other organization *(corporate author)* issuing the report.

2a. REPORT SECURITY CLASSIFICATION: Enter the overall security classification of the report. Indicate whether "Restricted Data" is included. Marking is to be in accordance with appropriate security regulations.

2b. GROUP: Automatic downgrading is specified in DoD Directive 5200.10 and Armed Forces Industrial Manual. Enter the group number. Also, when applicable, show that optional markings have been used for Group 3 and Group 4 as authorized.

3. REPORT TITLE: Enter the complete report title in all capital letters. Titles in all cases should be unclassified. If a meaningful title cannot be selected without classification, show title classification in all capitals in parenthesis immediately following the title.

4. DESCRIPTIVE NOTES: If appropriate, enter the type of report, e.g., interim, progress, summary, annual, or final. Give the inclusive dates when a specific reporting period is covered.

5. AUTHOR(S): Enter the name(s) of author(s) as shown on or in the report. Enter last name, first name, middle initial. If military, show rank and branch of service. The name of the principal author is an absolute minimum requirement.

6. REPORT DATE: Enter the date of the report as day, month, year; or month, year. If more than one date appears on the report, use date of publication.

7a. TOTAL NUMBER OF PAGES: The total page count should follow normal pagination procedures, i.e., enter the number of pages containing information.

7b. NUMBER OF REFERENCES: Enter the total number of references cited in the report.

8a. CONTRACT OR GRANT NUMBER: If appropriate, enter the applicable number of the contract or grant under which the report was written.

8b, 8c, & 8d. PROJECT NUMBER: Enter the appropriate military department identification, such as project number, subproject number, system numbers, task number, etc.

9a. ORIGINATOR'S REPORT NUMBER(S): Enter the official report number by which the document will be identified and controlled by the originating activity. This number must be unique to this report.

9b. OTHER REPORT NUMBER(S): If the report has been assigned any other report numbers *(either by the originator or by the sponsor)*, also enter this number(s).

10. AVAILABILITY/LIMITATION NOTICES: Enter any limitations on further dissemination of the report, other than those imposed by security classification, using standard statements such as:

(1) "Qualified requesters may obtain copies of this report from DDC."

(2) "Foreign announcement and dissemination of this report by DDC is not authorized."

(3) "U. S. Government agencies may obtain copies of this report directly from DDC. Other qualified DDC users shall request through _____."

(4) "U. S. military agencies may obtain copies of this report directly from DDC. Other qualified users shall request through _____."

(5) "All distribution of this report is controlled. Qualified DDC users shall request through _____."

If the report has been furnished to the Office of Technical Services, Department of Commerce, for sale to the public, indicate this fact and enter the price, if known.

11. SUPPLEMENTARY NOTES: Use for additional explanatory notes.

12. SPONSORING MILITARY ACTIVITY: Enter the name of the departmental project office or laboratory sponsoring *(paying for)* the research and development. Include address.

13. ABSTRACT: Enter an abstract giving a brief and factual summary of the document indicative of the report, even though it may also appear elsewhere in the body of the technical report. If additional space is required, a continuation sheet shall be attached.

It is highly desirable that the abstract of classified reports be unclassified. Each paragraph of the abstract shall end with an indication of the military security classification of the information in the paragraph, represented as *(TS), (S), (C), or (U)*.

There is no limitation on the length of the abstract. However, the suggested length is from 150 to 225 words.

14. KEY WORDS: Key words are technically meaningful terms or short phrases that characterize a report and may be used as index entries for cataloging the report. Key words must be selected so that no security classification is required. Identifiers, such as equipment model designation, trade name, military project code name, geographic location, may be used as key words but will be followed by an indication of technical context. The assignment of links, roles, and weights is optional.

David Taylor Model Basin. Report 2049.
A COMPARISON OF THE LIFTING-SURFACE CORRECTIONS CALCULATED BY DIFFERENT METHODS FOR THREE PROPELLER DESIGNS, by Ernest E. Harley. Sep 1965. v, 58p. illus., graphs, diags, tables, refs. UNCLASSIFIED

This report presents the results of a comparison of ligting-surface corrections calculated by several numerical methods for three propellers. Specifically, the camber corrections, radial and chordwise distribution of camber, and the propeller pitch ratios are compared. The results of the comparison, presented in non-dimensional form, are shown graphically and through tables.

1. Propellers--Design--Mathematical analysis
2. Propellers--Design--Hydrodynamic aspects
3. Lifting surfaces--Theory
I. Harley, Ernest E.
II. S-R009 01 01; Task 0101

David Taylor Model Basin. Report 2049.
A COMPARISON OF THE LIFTING-SURFACE CORRECTIONS CALCULATED BY DIFFERENT METHODS FOR THREE PROPELLER DESIGNS, by Ernest E. Harley. Sep 1965. v, 58p. illus., graphs, diags, tables, refs. UNCLASSIFIED

This report presents the results of a comparison of ligting-surface corrections calculated by several numerical methods for three propellers. Specifically, the camber corrections, radial and chordwise distribution of camber, and the propeller pitch ratios are compared. The results of the comparison, presented in non-dimensional form, are shown graphically and through tables.

1. Propellers--Design--Mathematical analysis
2. Propellers--Design--Hydrodynamic aspects
3. Lifting surfaces--Theory
I. Harley, Ernest E.
II. S-R009 01 01; Task 0101

David Taylor Model Basin. Report 2049.
A COMPARISON OF THE LIFTING-SURFACE CORRECTIONS CALCULATED BY DIFFERENT METHODS FOR THREE PROPELLER DESIGNS, by Ernest E. Harley. Sep 1965. v, 58p. illus., graphs, diags, tables, refs. UNCLASSIFIED

This report presents the results of a comparison of ligting-surface corrections calculated by several numerical methods for three propellers. Specifically, the camber corrections, radial and chordwise distribution of camber, and the propeller pitch ratios are compared. The results of the comparison, presented in non-dimensional form, are shown graphically and through tables.

1. Propellers--Design--Mathematical analysis
2. Propellers--Design--Hydrodynamic aspects
3. Lifting surfaces--Theory
I. Harley, Ernest E.
II. S-R009 01 01; Task 0101